Article

Cell Reports

A Specific ChREBP and PPARα Cross-Talk Is Required for the Glucose-Mediated FGF21 Response

Graphical Abstract

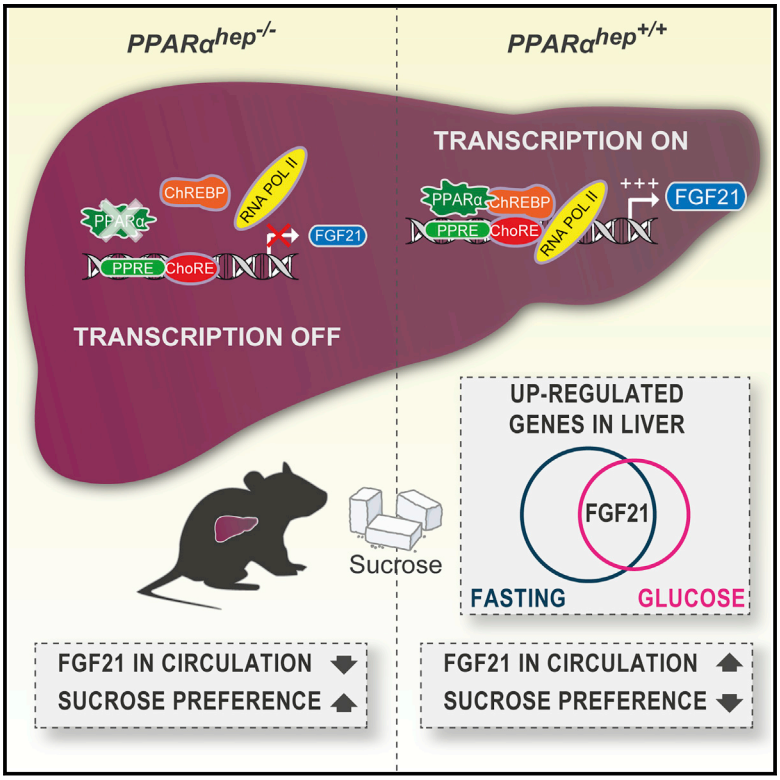

Highlights

- *Fgf21* is a unique hepatic gene inducible by both catabolic and anabolic signals
- The ChREBP-mediated induction of *Fgf21* in hepatocytes requires PPARα
- Loss of PPARα impairs *Fgf21* promoter accessibility at the ChoRE
- PPARα is required for the control of sucrose preference in vivo

Authors

Alison Iroz, Alexandra Montagner, Fadila Benhamed, ..., Renaud Dentin, Hervé Guillou, Catherine Postic

Correspondence

renaud.dentin@inserm.fr (R.D.), herve.guillou@inra.fr (H.G.), catherine.postic@inserm.fr (C.P.)

In Brief

FGF21 is a hepatokine with beneficial metabolic effects, including control of sucrose preference. Iroz et al. demonstrate that *Fgf21* is a unique hepatic gene inducible by both fasting and glucose signals and that the transcription factors PPARα and ChREBP both regulate the endocrine control of sugar intake by hepatic FGF21.

Data and Software Availability

GSE92502

Iroz et al., 2017, Cell Reports *21*, 403–416
October 10, 2017
https://doi.org/10.1016/j.celrep.2017.09.065

Cell Reports
Article

A Specific ChREBP and PPARα Cross-Talk Is Required for the Glucose-Mediated FGF21 Response

Alison Iroz,[1,2,3,10] Alexandra Montagner,[4,10] Fadila Benhamed,[1,2,3,10] Françoise Levavasseur,[1,2,3] Arnaud Polizzi,[4] Elodie Anthony,[1,2,3] Marion Régnier,[4] Edwin Fouché,[4] Céline Lukowicz,[4] Michèle Cauzac,[1,2,3] Emilie Tournier,[1,2,3] Marcio Do-Cruzeiro,[1,2,3] Martine Daujat-Chavanieu,[5,6,7] Sabine Gerbal-Chalouin,[5,6,7] Véronique Fauveau,[1,2,3] Solenne Marmier,[1,2,3] Anne-Françoise Burnol,[1,2,3] Sandra Guilmeau,[1,2,3] Yannick Lippi,[4] Jean Girard,[1,2,3] Walter Wahli,[4,8,9] Renaud Dentin,[1,2,3,11,*] Hervé Guillou,[4,11,*] and Catherine Postic[1,2,3,11,12,*]
[1]INSERM U1016, Institut Cochin, Paris 75014, France
[2]CNRS UMR 8104, Paris 75014, France
[3]University of Paris Descartes, Sorbonne Paris Cité, Paris 75005, France
[4]Toxalim, Université de Toulouse, INRA, ENVT, INP-Purpan, UPS, Toulouse 31027, France
[5]INSERM, U1183, Institute for Regenerative Medicine and Biotherapy, Montpellier, France
[6]Université de Montpellier, UMR 1183, Montpellier, France
[7]CHU Montpellier, Institute for Regenerative Medicine and Biotherapy, Montpellier, France
[8]Lee Kong Chian School of Medicine, Nanyang Technological University, Singapore 308232, Singapore
[9]Center for Integrative Genomics, University of Lausanne, Genopode Building, Lausanne 1015, Switzerland
[10]These authors contributed equally
[11]Senior author
[12]Lead Contact
*Correspondence: renaud.dentin@inserm.fr (R.D.), herve.guillou@inra.fr (H.G.), catherine.postic@inserm.fr (C.P.)
https://doi.org/10.1016/j.celrep.2017.09.065

SUMMARY

While the physiological benefits of the fibroblast growth factor 21 (FGF21) hepatokine are documented in response to fasting, little information is available on *Fgf21* regulation in a glucose-overload context. We report that peroxisome-proliferator-activated receptor α (PPARα), a nuclear receptor of the fasting response, is required with the carbohydrate-sensitive transcription factor carbohydrate-responsive element-binding protein (ChREBP) to balance FGF21 glucose response. Microarray analysis indicated that only a few hepatic genes respond to fasting and glucose similarly to *Fgf21*. Glucose-challenged *Chrebp*$^{-/-}$ mice exhibit a marked reduction in FGF21 production, a decrease that was rescued by re-expression of an active ChREBP isoform in the liver of *Chrebp*$^{-/-}$ mice. Unexpectedly, carbohydrate challenge of hepatic *Pparα* knockout mice also demonstrated a PPARα-dependent glucose response for *Fgf21* that was associated with an increased sucrose preference. This blunted response was due to decreased *Fgf21* promoter accessibility and diminished ChREBP binding onto *Fgf21* carbohydrate-responsive element (ChoRE) in hepatocytes lacking PPARα. Our study reports that PPARα is required for the ChREBP-induced glucose response of FGF21.

INTRODUCTION

The liver is central for the regulation of energy homeostasis, controlling several biochemical pathways important for metabolism of lipids, carbohydrates, proteins, bile synthesis, and detoxification of drugs and toxins. The liver also controls endocrine responses through the production of hepatokines. These proteins secreted by the hepatocytes act as hormones, and several hepatokines are considered promising leads for metabolic therapy development (Iroz et al., 2015). Among them, fibroblast growth factor 21 (FGF21) has emerged as an interesting target (Kharitonenkov and Adams, 2013). Originally targeted for its glucose-lowering properties in rodents and primates (Berglund et al., 2009; Fisher et al., 2011; Kharitonenkov et al., 2007), FGF21 is also able to improve insulin sensitivity and lipid homeostasis and induce weight loss (Coskun et al., 2008; Markan et al., 2014).

Fgf21 is a direct target of the nuclear receptor peroxisome-proliferator-activated receptor α (PPARα) in response to fasting (Badman et al., 2007; Lundåsen et al., 2007). Activated by free fatty acids derived from lipolysis (Jaeger et al., 2015; Montagner et al., 2016), PPARα is essential to liver health, as its deletion promotes the development of non-alcoholic fatty liver disease (NAFLD) and hypercholesterolemia during aging (Montagner et al., 2016). The beneficial role of PPARα in response to dyslipidemia is thought to be mediated, at least in part, through FGF21 (Ong et al., 2012). Indeed, anti-diabetic therapies and PPARα agonists (fenofibrate or Wy-14653) significantly induce liver-derived FGF21 in both mouse and human plasma (Christodoulides et al., 2009; Gälman et al., 2008; Lundåsen et al., 2007).

Hepatocyte PPARα plays an essential role during fasting, which triggers transcriptional regulation for the maintenance of glycemia and ketogenesis through fatty acid catabolism for use as an alternative energy source (Goldstein and Hager, 2015). In agreement, PPARα-deficient mice exhibit impaired fatty acid oxidation and ketogenesis that promotes hepatic steatosis during fasting (Kersten et al., 1999; Kroetz et al., 1998; Leone et al., 1999; Montagner et al., 2016).

Recent work reported that FGF21 is also activated in response to glucose and fructose in rodents and humans (Herman et al., 2012; Iizuka et al., 2009; Sánchez et al., 2009; Uebanso et al., 2011). Enriched in liver, the transcription factor carbohydrate-responsive element-binding protein (ChREBP) mediates the response to dietary carbohydrates (Abdul-Wahed et al., 2017). A physiological role for the ChREBP-FGF21 axis was revealed in experiments showing that in response to sugar consumption, ChREBP-enhanced FGF21 secretion from the liver blocked sugar-seeking behavior in mice and primates by targeting the paraventricular nucleus of the hypothalamus (Talukdar et al., 2016; von Holstein-Rathlou et al., 2016). The ChREBP protein contains a low-glucose inhibitory domain (LID) and a glucose responsive activation conserved element (*GRACE*) located in its N terminus (Li et al., 2006). Activation of GRACE by glucose promotes ChREBP transcriptional activity and binding to the carbohydrate-responsive element (ChoRE) of its target genes, including L-pyruvate kinase (*Lpk*), a rate-limiting enzyme in glycolysis, fatty acid synthase (*Fas*), and steroyl CoA desaturase (*Scd1*), key enzymes of de novo lipogenesis (Kawaguchi et al., 2001). Another isoform of *Chrebp*, *Chrebp*β, originating from an alternative promoter, was identified in adipose tissue and liver (Herman et al., 2012). This alternative splicing results in a constitutively active ChREBP isoform lacking the LID, a domain associated with inhibition of ChREBP activity (Herman et al., 2012).

Understanding the regulation of FGF21 is currently a research focal point. Through the use of *Chrebp* knockout mice, we report here that ChREBP is required for the expression and secretion of hepatic FGF21 in response to carbohydrate intake. Unexpectedly, studies in hepatocyte-specific *Ppar*α knockout mice reveal a physiological role for PPARα in the context of glucose challenge, as ChREBP is unable to induce *Fgf21* in the absence of hepatic PPARα. Altogether, our results suggest that FGF21's glucose-mediated response is dependent on both ChREBP and PPARα.

RESULTS

FGF21 Is Induced by Both Fasting and Glucose Challenge

To characterize gene expression during fasting and a glucose challenge, a microarray analysis was conducted using liver samples from wild-type mice (Figure 1). Genes sensitive to glucose or fasting that were markedly different from the fed group were incorporated into a heatmap (Figure 1A). 67 genes were significantly induced by glucose in comparison to fed conditions (cluster 1), and 675 genes were significantly upregulated between fed and fasted groups (cluster 6). Gene ontology analysis revealed that pathways identified as specifically impacted by glucose and not by fasting are involved in pyruvate and insulin-sensitive metabolism (Figure 1B). Gene ontology revealed that pathways specifically sensitive to fasting, but not to glucose, are involved in PPAR signaling (Figure 1C). Interestingly, among the top genes upregulated by glucose and fasting (Figure S1A), only 3 genes (*Fgf21*, *Fut1*, and *Atf5*) were significantly upregulated (log fold change [FC] > 1; $p \leq 0.01$) as compared to fed conditions (Figure 1D). When the stringency of the selection was increased to a log FC > 2 (Figure 1E), *Fgf21* was left to be the sole gene upregulated by both fasting and glucose challenge (log FC = 3.9 and log FC = 3.7, respectively ($p \leq 0.01$) (Figure 1E). qPCR analysis confirmed that *Fgf21* expression was significantly upregulated by fasting and glucose compared to fed conditions (Figure 1F). The glucose effect was validated through analysis of *Chrebp*, *Chrebp*β, and *Lpk* gene expression, while the effect of fasting was assessed by measuring the expression of two typical PPARα targets, *Cyp4a10* and *Vnn1* (Figure 1F).

ChREBP Is Necessary for Glucose-Mediated Expression and Secretion of Hepatic FGF21

To address the importance of ChREBP in the *Fgf21* glucose response, experiments were first performed in mouse hepatocytes from wild-type mice (Figure 2). We observed that *Fgf21* expression was induced by elevated glucose concentrations and paralleled with *Chrebp*, *Chrebp*β, and target gene expression (Figure 2A). ChREBP recruitment onto the *Fgf21* and *Lpk* promoters significantly increased under high glucose concentrations (25 mM) (Figure 2B). This stimulatory effect of glucose was specific and not linked to an osmotic shock, since *Fgf21* expression was not induced in response to mannitol (Figure S2). To determine whether ChREBP is mandatory for upregulation of FGF21 in response to glucose, experiments were completed in hepatocytes lacking ChREBP ($Chrebp^{-/-}$) (Figures 2C–2E). Mice lacking exons 9–15 of the *Chrebp* gene were generated through homologous recombination (Figure S3). The absence of the ChREBP protein (α isoform, 94 kDa) was validated in $Chrebp^{-/-}$ hepatocytes by western blot analysis (Figure 2C). Under these conditions, the ChREBPβ protein (72 kDa) could not be detected (data not shown). Similarly to *Chrebp, Chrebp*β, and the ChREBP and ChREBPβ target genes *Lpk* and *Scd1*, *Fgf21* robustly responded to 25 mM glucose stimulation in wild-type hepatocytes, but this response was blunted in $Chrebp^{-/-}$ hepatocytes (Figure 2D). In addition, no increase in FGF21 in culture medium was detected when $Chrebp^{-/-}$ hepatocytes were cultured in 25 mM glucose (Figure 2E). Of note, basal FGF21 production (5 mM glucose) was also significantly decreased in culture medium from $Chrebp^{-/-}$ hepatocytes (Figure 2E). These findings indicate that ChREBP is mandatory for the glucose-mediated expression and secretion of FGF21 by hepatocytes.

Liver-Specific ChREBP Expression Rescues FGF21 Plasma Concentrations in ChREBP Knockout Mice

We next performed glucose challenge experiments in vivo. 10- to 12-week-old $Chrebp^{+/+}$ and $Chrebp^{-/-}$ male mice were given 24-hr access to a bottle of glucose-free water (fed) or a bottle containing 20% glucose (glucose challenge) (Figure 3). A significant elevation in blood glucose was observed in glucose-challenged $Chrebp^{-/-}$ mice compared to $Chrebp^{+/+}$ mice under the same conditions (Figure 3A). A trend toward higher insulin concentrations was observed in $Chrebp^{-/-}$ mice compared to controls (under fed and glucose conditions), but this difference did not reach statistical significance (Figure 3B). Glucose challenge raised ChREBP protein content in liver of $Chrebp^{+/+}$ mice (Figure 3C). A significant stimulation in hepatic triglyceride (TG) concentrations was also observed in glucose-challenged $Chrebp^{+/+}$ mice, but not $Chrebp^{-/-}$ mice (Figure 3D).

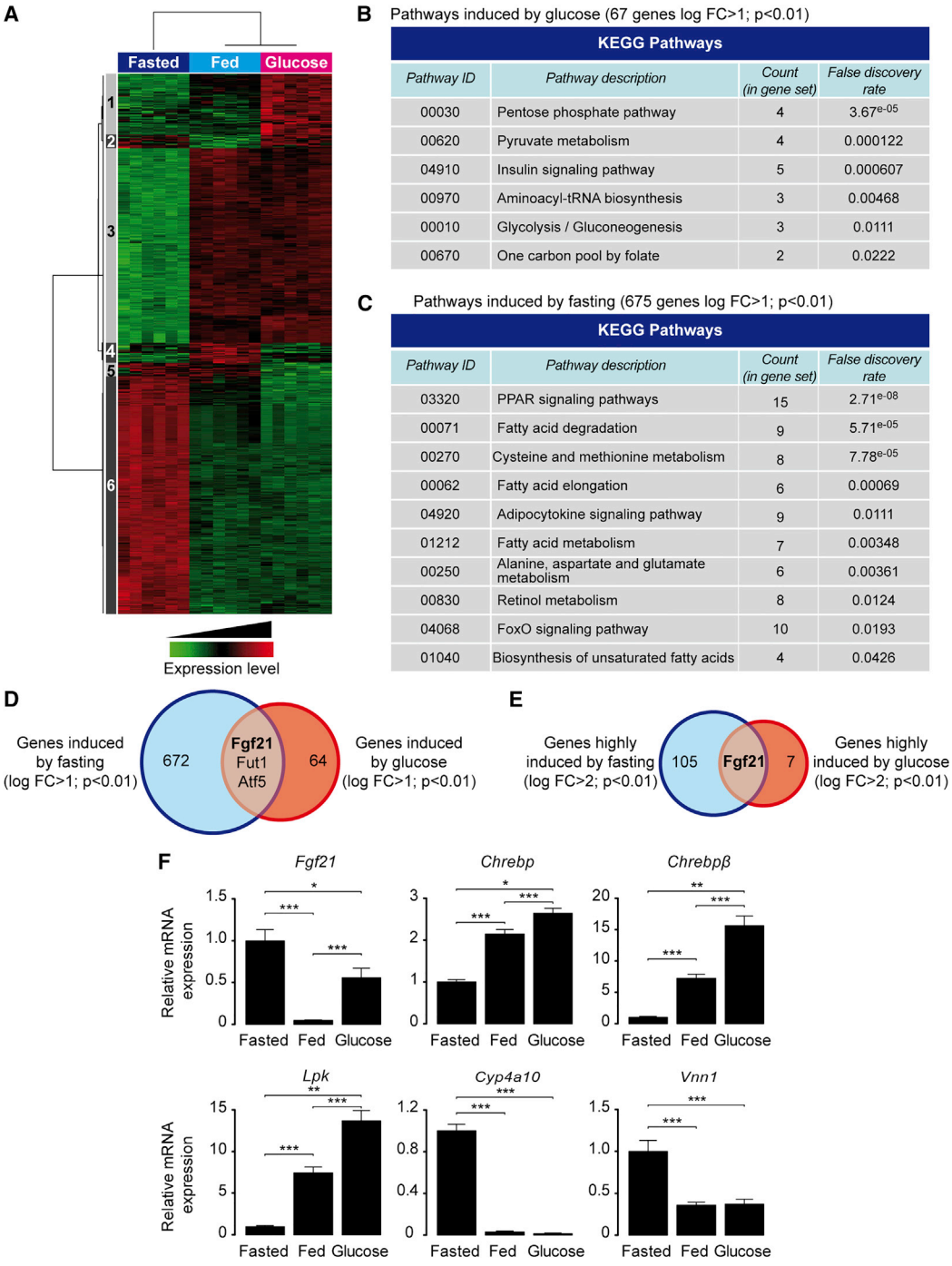

Figure 1. FGF21 Is Highly Induced by Both Fasting and Glucose Challenge

Wild-type C57BL/6J 10-week-old male mice were fed ad libitum, fasted for 24 hr, or fed for 24 hr a standard diet with addition of 20% glucose in drinking water (glucose challenge). Mice were killed at ZT14 (14 hr after the start of light period in the animal housing unit). Transcriptomic analysis was performed on livers (n = 6 per condition) using gene expression microarray.

(A) Heatmap of differentially expressed probes (false discovery rate [FDR] < 5%).

(B and C) KEGG categories corresponding to functions impacted by glucose (B) and fasting (C).

(D) Venn diagram presenting the overlap between glucose- and fasting-induced gene expression (log FC > 1; adjusted p < 0.01).

(E) Venn diagram presenting the overlap between glucose- and fasting-induced gene expression (log FC > 2; adjusted p < 0.01).

(F) Gene expression determined by qPCR. Data are expressed as means ± SEM, n = 6 individual mice per group. Significance is based on two-way ANOVA followed by a Bonferroni post hoc test. *p < 0.05, **p < 0.01, ***p < 0.001.

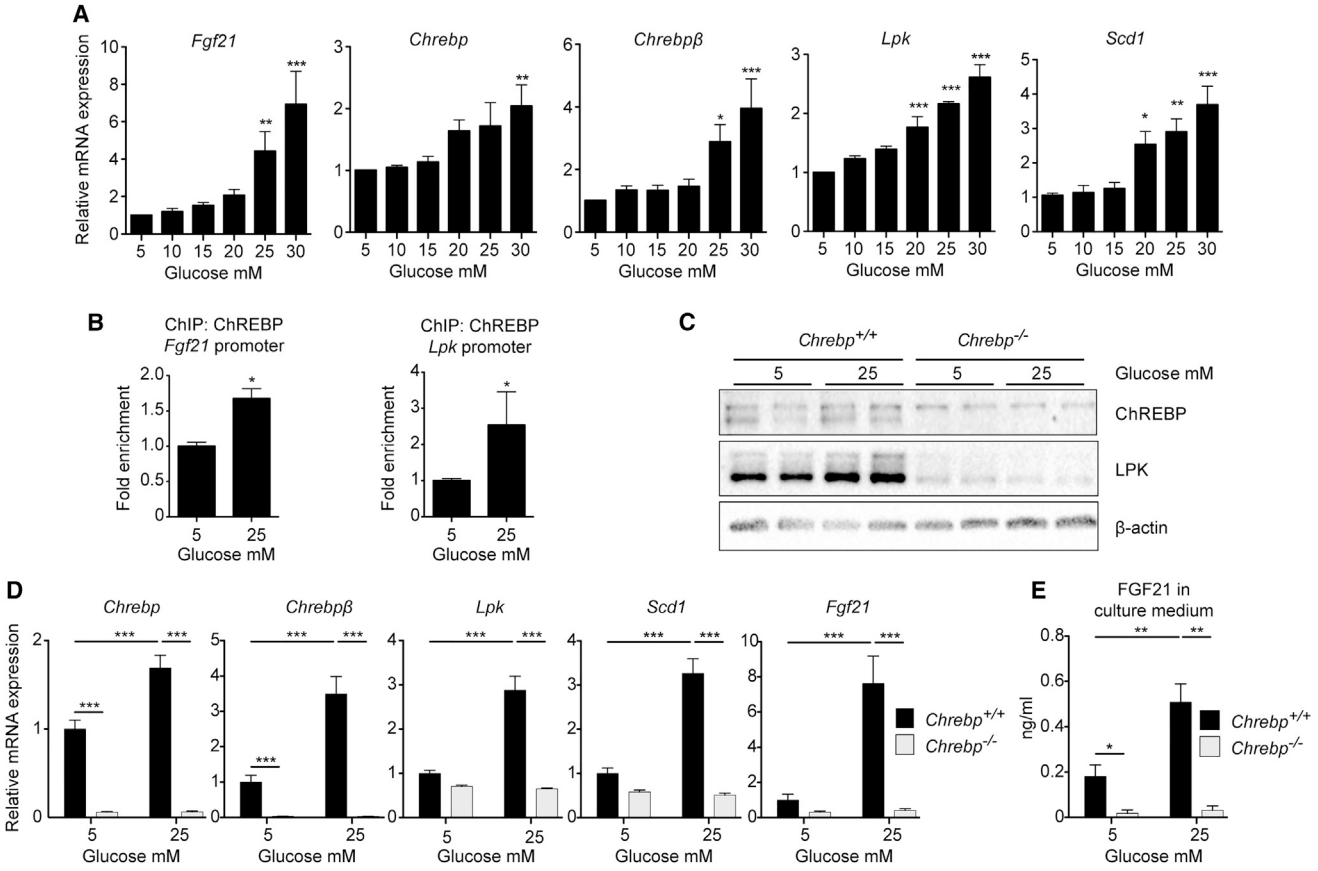

Figure 2. ChREBP Is Necessary for Glucose-Mediated Expression and Secretion of FGF21 In Vitro

(A and B) Hepatocytes prepared from male C57BL/6J mouse livers were stimulated 1 day after platting for 24 hr with medium containing 5, 10, 15, 20, 25, or 30 mM glucose. (A) qPCR analysis of *Fgf21*, *Chrebp, Chrebpβ, Lpk*, and *Scd1* gene expression. Data are presented as means ± SEM from 4 independent cultures done in triplicate. Significance is based on two-way ANOVA followed by a Bonferroni post hoc test (*p < 0.05; **p < 0.01; ***p < 0.001). (B) ChIP analysis for ChREBP binding on the *Fgf21* and *Lpk* ChoRE followed by qPCR in mouse hepatocytes challenged with 5 or 25 mM glucose for 24 hr. Data are expressed as means ± SEM (n = 3). Significance is based on Student's t test followed by Mann-Whitney post hoc test (*p < 0.05).

(C–E) Primary hepatocytes from female *Chrebp*$^{-/-}$ and *Chrebp*$^{+/+}$ littermates were stimulated 1 day after platting for 24 hr with cell culture medium containing 5 or 25 mM glucose. (C) Western blot analysis of protein from whole hepatocyte lysate. Two representative samples are presented. β actin was used as loading control. (D) Gene expression determined by qPCR. (E) ELISA quantification of FGF21 protein in medium collected at the end of glucose stimulation.

Data are presented as means ± SEM from 4 independent cultures in triplicate. Significance is based on two-way ANOVA followed by a Bonferroni post hoc test (*p < 0.05; **p < 0.01; ***p < 0.001).

A significant increase in *Chrebp*, *Chrebpβ*, *Lpk*, and *Scd1* mRNA levels was observed in liver of glucose-challenged *Chrebp*$^{+/+}$ mice compared to fed mice from the same genotype (Figure 3E). *Fgf21* mRNA and plasmatic FGF21 protein concentrations markedly increased in glucose-challenged *Chrebp*$^{+/+}$ mice. While a residual (nonsignificant) glucose effect was observed in *Chrebp*$^{-/-}$ mice, this response was significantly reduced compared to *Chrebp*$^{+/+}$ mice (Figures 3F and 3G), despite elevated blood glucose levels (Figure 3A). These results show that ChREBP is required for the in vivo glucose-mediated induction of *Fgf21*.

We next addressed whether liver-specific re-expression of *Chrebp* in a context of global ChREBP deficiency could rescue FGF21 production. *Chrebp*$^{+/+}$ and *Chrebp*$^{-/-}$ adult mice were injected with an adenovirus vehicle containing the GFP protein or a truncated isoform of ChREBP lacking the LID domain (Li et al., 2006) corresponding to a constitutively active ChREBP isoform (ChREBP^{CA}). Mice received a 20% glucose solution for 24 hr before sacrifice (Figures 3H–3K). Blood glucose concentrations were higher in GFP-ChREBP$^{-/-}$ mice than in GFP-ChREBP$^{+/+}$ mice and were rescued to basal values when ChREBP^{CA} was injected into *Chrebp*$^{-/-}$ mice (Figure 3H). Western blot analysis confirmed the absence of native ChREBP protein (94 kDa) but the presence of ChREBP^{CA} (72 kDa) in *Chrebp*$^{-/-}$ mice injected with ChREBP^{CA} (Figure 3I). Importantly, ChREBP^{CA} rescued the circulating level of FGF21 (Figure 3J). This correlates with the effect of ChREBP^{CA} on the hepatic expression of *Chrebp*, *Chrebpβ*, and their targets, *Lpk, Scd1*, and *Fgf21* mRNA (Figure 3K). Altogether, we report that ChREBP^{CA} administration rescued ChREBP activity in the liver of *Chrebp*$^{-/-}$ mice and was sufficient to restore FGF21 gene expression and production.

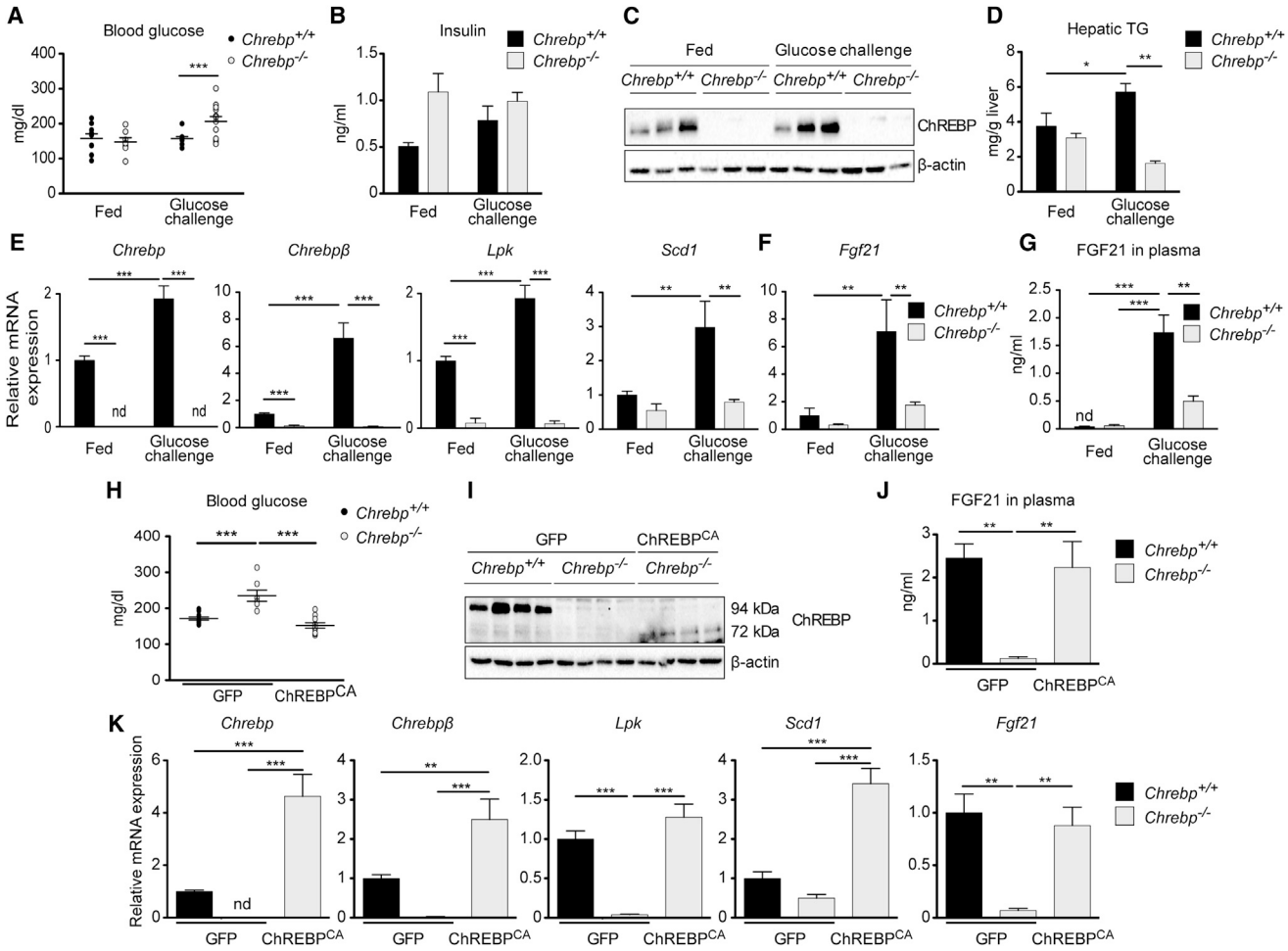

Figure 3. FGF21 Is Unable to Respond to a Glucose Challenge without ChREBP

(A–G) Adult male *Chrebp*$^{-/-}$ and *Chrebp*$^{+/+}$ littermates were allowed access to a 20% glucose drinking water solution and standard chow diet ad libitum for 18 hr. Fed mice received drinking water from the same water source used to make the glucose solution. (A) Blood glucose (mg/dl) recovered at the time of harvest from tail snip. (B) Insulin concentrations (ng/ml). (C) Western blot analysis of protein from whole liver lysate. β actin was used as loading control. Three representative samples are presented. (D) Hepatic triglyceride (TG) concentrations. Relative *Chrebp*, *Chrebpβ*, *Lpk*, and *Scd1* gene expression (E) and *Fgf21* (F) gene expression determined by qPCR. (G) ELISA quantification of FGF21 protein (ng/mL) in plasma. Data are presented as means ± SEM from 6 to 8 individual mice. Significance is based on two-way ANOVA followed by a Bonferroni post hoc test (*$p < 0.05$; **$p < 0.01$; ***$p < 0.001$; nd, not detectable).

(H–J) Adult male *Chrebp*$^{+/+}$ and *Chrebp*$^{-/-}$ mice were injected intravenously with a single dose of 3×10^9 pfu GFP or ChREBP^{CA} adenovirus on day 1. Four days later, analyses were performed. (H) Blood glucose (mg/dl) recovered at the time of harvest from tail snip. (I) Western blot analysis of protein extracted from whole liver lysate. β actin was used as loading control. Three representative samples are presented. (J) ELISA quantification of FGF21 protein (ng/ml) in plasma.

(K) Relative expression of hepatic genes determined by qPCR.

Data are presented as means ± SEM from 8 to 12 individual mice. Significance is based on two-way ANOVA followed by a Bonferroni post hoc test (*$p < 0.05$; **$p < 0.01$; ***$p < 0.001$; nd, not detectable).

Glucose Stimulation or ChREBP Overexpression Is Not Efficient to Induce FGF21 Expression or Secretion in the Absence of Hepatic PPARα

Since the *Fgf21* promoter contains overlapping peroxisome proliferator response element (PPRE) and ChoRE units (−88 to −54 bp) (Girer et al., 2016; Uebanso et al., 2011), we investigated whether PPARα could impact the glucose response of *Fgf21* mediated by *Chrebp*. Primary hepatocytes from liver-specific *Pparα* knockout mice (*Pparα*$^{hep-/-}$) and their littermates, *Pparα*$^{hep\ +/+}$ mice (Montagner et al., 2016), were stimulated by glucose in a dose-dependent manner (Figure 4). A similar glucose-mediated induction of *Chrebp*, *Chrebpβ*, *Lpk*, and *Scd1* mRNA was observed in hepatocytes from *Pparα*$^{hep\ +/+}$ and *Pparα*$^{hep\ -/-}$ mice (Figure 4A). Although a residual glucose effect was observed for *Fgf21* expression in *Pppaα*$^{hep\ -/-}$ mice hepatocytes, this response was reduced compared to *Pparα*$^{hep+/+}$ mice (Figure 4B). Importantly, FGF21 production in response to glucose was reduced by 60% in culture medium from *Pppaα*$^{hep-/-}$ hepatocytes compared to controls (Figure 4C). This profile was specific to *Fgf21*, since the expression of other typical PPARα targets (*Cyp4a10*, *Cyp4a14*, or *Vnn1*) was not induced by glucose (Figure S4). We

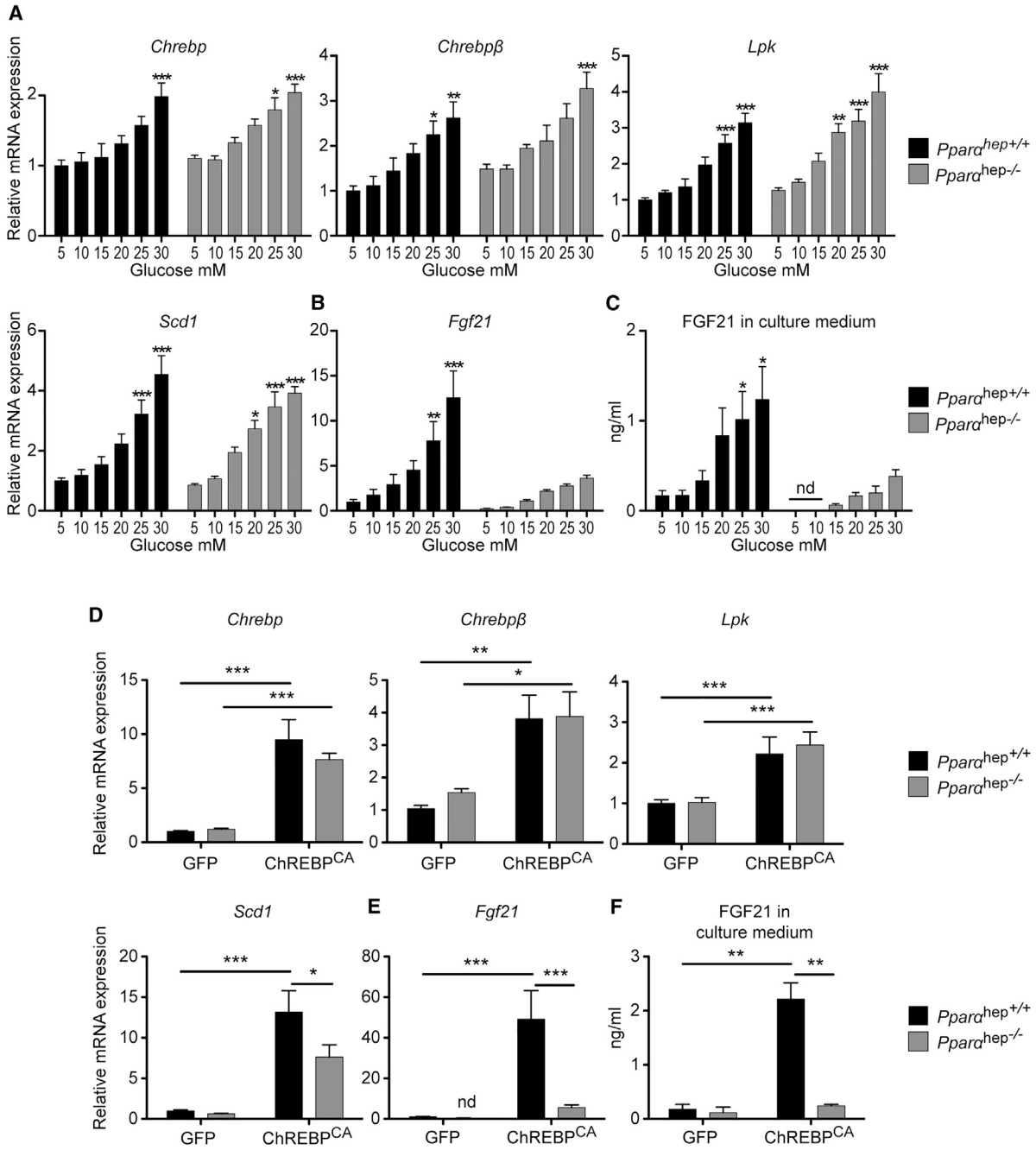

Figure 4. *Fgf21* Is Not Efficiently Induced by Glucose or by ChREBP Overexpression in the Absence of Liver PPARα

(A–C) Primary hepatocytes derived from adult male *Pparα*$^{hep+/+}$ or *Pparα*$^{hep-/-}$ mice were incubated 1 day after platting for 24 hr with medium containing 5, 10, 15, 20, 25, or 30 mM glucose. Relative *Chrebp, Chrebpβ*, *Lpk*, and *Scd1* gene expression (A) and *Fgf*21 gene expression (B) was determined by qPCR. (C) ELISA quantification of FGF21 protein (ng/ml) in medium collected at end of glucose stimulation. Figures are presented as means ± SEM from 4 independent cultures completed in duplicate. Significance is based on two-way ANOVA followed by a Bonferroni post hoc test (*p < 0.05; **p < 0.01; ***p < 0.001; nd, not detectable).

(D–F) Primary hepatocytes derived from adult male mice *Pparα*$^{hep+/+}$ or *Pparα*$^{hep-/-}$ were incubated 6 hr after platting with 3 × 10^9 pfu GFP or ChREBP^{CA} adenovirus at a glucose concentration of 5 mM for 24 hr. Relative *Chrebp*, *Chrebpβ*, *Lpk*, and *Scd1* expression (D) and of *Fgf*21 expression (E) was determined by qPCR. (F) ELISA quantification of FGF21 protein (in ng/ml) in medium collected at end of adenoviral treatment.

Data are presented as means ± SEM from 4 independent cultures completed in duplicate. Significance is based on two-way ANOVA followed by a Bonferroni post hoc test (*p < 0.05; **p < 0.01; ***p < 0.001).

next addressed whether *Fgf21* could be rescued by *Chrebp* overexpression in the context of *Pparα* deficiency. Hepatocytes from *Pparα*$^{hep+/+}$ and *Pppaα*$^{hep\ -/-}$ mice were infected with the constitutive active form of ChREBP (ChREBP^{CA}) for 24 hr. The expression of *Chrebp* and *Chrebpβ* was significantly increased in response to ChREBP^{CA} in both *Pparα* $^{hep+/+}$ and *Pppaα*$^{hep\ -/-}$ hepatocytes, and as a result, *Lpk* and *Scd1* mRNA expression was stimulated compared to GFP conditions (Figure 4D). However, while *Chrebp* overexpression led to a 50-fold increase in *Fgf21* expression in *Pparα*$^{hep+/+}$ hepatocytes, it failed to significantly induce *Fgf21* expression in *Pppaα*$^{hep\ -/-}$ hepatocytes (Figure 4E). FGF21 measured in the medium of cell culture confirmed the *Fgf21* mRNA expression profile (Figure 4F). These results suggest that neither glucose nor ChREBP overexpression is efficient in inducing *Fgf21* gene expression or protein production in the absence of PPARα in hepatocytes.

FGF21 Synergistically Responds to Glucose and a Pharmacological PPARα Activator in Both Mouse and Human Hepatocytes

To determine whether ChREBP and PPARα act in synergy to regulate *Fgf21* gene expression, mouse and human hepatocytes were stimulated for 24 hr with low (5 mM) or high glucose concentrations (25 mM) in the presence of the PPARα agonist Wy-14643 (Figure S5). Expression of *Chrebp* and *Chrebpβ* mRNA confirmed a positive glucose response in both mouse and human hepatocytes (Figures S5A and S5B). Activation of PPARα by Wy-14643 was validated by a significant upregulation in *Acox1* expression, a PPARα target gene (Figures S5C and S5D). *Fgf21* mRNA levels were drastically increased when hepatocytes (mouse and human) were incubated in the combined presence of high glucose (25 mM) and Wy-14643 (Figures S5E and S5F). Altogether, these results show that ChREBP and PPARα can act synergistically to induce *Fgf21* in mouse and in human liver cells.

Hepatocyte PPARα Is Required for the Effect of Glucose on FGF21 In Vivo

To investigate whether PPARα is involved in the glucose-mediated induction of *Fgf21* in vivo, glucose challenge experiments were performed in 10- to 12-week-old *Pparα*$^{hep+/+}$ and *Pparα* $^{hep-/-}$ mice. Three nutritional conditions were assigned to both genotypes: (1) mice fasted 24 hr with free access to water (fasted), (2) mice fed ad libitum with access to standard chow diet and free access to water (fed), and (3) mice fed ad libitum with access to standard chow diet and a 20% glucose solution in water (glucose challenge) (Figure 5). *Chrebp*, *Chrebpβ*, and their target genes (*Lpk* and *Scd1*) were induced in a similar manner in the liver of *Pparα* $^{hep+/+}$ and *Pparα*$^{hep-/-}$ mice when challenged by glucose (Figure 5A). In contrast, the glucose-mediated induction of *Fgf21* (compared to the fed state) was significantly reduced in the absence of PPARα (Figure 5A). FGF21 in the circulation matched hepatic mRNA levels, revealing an upregulation of FGF21 in the plasma of *Pparα* $^{hep+/+}$ that was significantly reduced in glucose-challenged *Pparα*$^{hep-/-}$ mice (Figure 5B). As expected, loss of PPARα markedly impacted the fasting response of FGF21 (Figure 5A-B). Because the *Fgf21* promoter contains overlapping PPRE and ChoRE units (Figure 5C), we investigated whether lack of PPARα could impair ChREBP binding in response to glucose in vivo. When primers amplifying both ChoRE and PPRE were used (Figure 5C), a significant enrichment in PPARα binding within the proximal region of the *Fgf21* promoter in liver of *Pparα* $^{hep+/+}$ mice was observed (Figure 5D). While PPARα binding was elevated under fasting conditions, a significant PPARα recruitment onto the proximal region of the *Fgf21* promoter was detected under both fed and glucose-challenge conditions (Figure 5D). Surprisingly, in liver of glucose challenged *Pparα* $^{hep-/-}$ mice, recruitment of ChREBP on the *Fgf21* promoter ChoRE was significantly reduced (Figure 5D). Interestingly, a significant decrease in RNA polymerase II (Pol II) recruitment and histone H3 lysine 9 acetylation (H3K9ac), a histone mark related to transcriptional activation, was observed in parallel in the liver of these mice (Figure 5D). In contrast, ChREBP recruitment on the *Lpk* ChoRE was similar in glucose-challenged *Pparα*$^{hep+/+}$ and *Pparα*$^{hep\ -/-}$ mice (Figure 5E). The presence of Pol II on the *Lpk* promoter (Figure 5E) was significantly elevated in response to glucose in liver of mice from both genotypes and correlated with *Lpk* mRNA expression (Figure 5A). Altogether, our results show that the absence of PPARα impairs the binding of ChREBP to its ChoRE and the subsequent glucose-mediated induction of *Fgf21*. Surprisingly, significant ChREBP recruitment was also detected on the *Fgf21* ChoRE under fasting conditions (Figure 5D). Further analysis will be required to determine whether ChREBP interferes with the fasting-mediated induction of *Fgf21* expression in the liver, as suggested in a recent report showing that liver-specific *Chrebp* knockout mice have decreased *Fgf21* expression compared to controls (Jois et al., 2017).

Fgf21 Promoter Accessibility Is Reduced in the Absence of PPARα

To provide insights into the mechanisms by which PPARα affects ChREBP binding onto the *Fgf21* promoter in response to glucose, a series of experiments were conducted in vitro (Figure 6). First, we performed formaldehyde-assisted isolation of regulatory elements (FAIRE)-qPCR analysis (Simon et al., 2012) to determine whether ChREBP accessibility to the *Fgf21* promoter could be altered in the absence of PPARα (Figure 6A). We observed that while *Fgf21* ChoRE promoter accessibility tended to increase in response to high glucose concentrations in *Pparα* $^{hep+/+}$ hepatocytes, it failed to increase in *Pparα* $^{hep-/-}$ hepatocytes (Figure 6A). To get insight into the molecular mechanisms involved, we hypothesized that PPARα could affect ChoRE accessibility through epigenetic processes and tested whether a pan-histone deacetylase (pan-HDAC) inhibitor (Imai et al., 2016) could increase *Fgf21* promoter accessibility. Treatment of hepatocytes with a HDAC inhibitor further enhanced the difference observed in *Fgf21* accessibility between *Pparα*$^{hep+/+}$ and *Pparα*$^{hep-/-}$ hepatocytes (Figure 6A), which correlated with a potentiated effect of glucose on *Fgf21* expression (Figure 6B). While no significant change in *Fgf21* promoter accessibility was observed in *Pparα*$^{hep\ -/-}$ hepatocytes treated with the HDAC inhibitor (Figure 6A), a modest but significant effect was observed for *Fgf21* mRNA levels measured under these conditions. However, treatment failed to fully rescue *Fgf21* gene expression to control levels (Figure 6B). These data

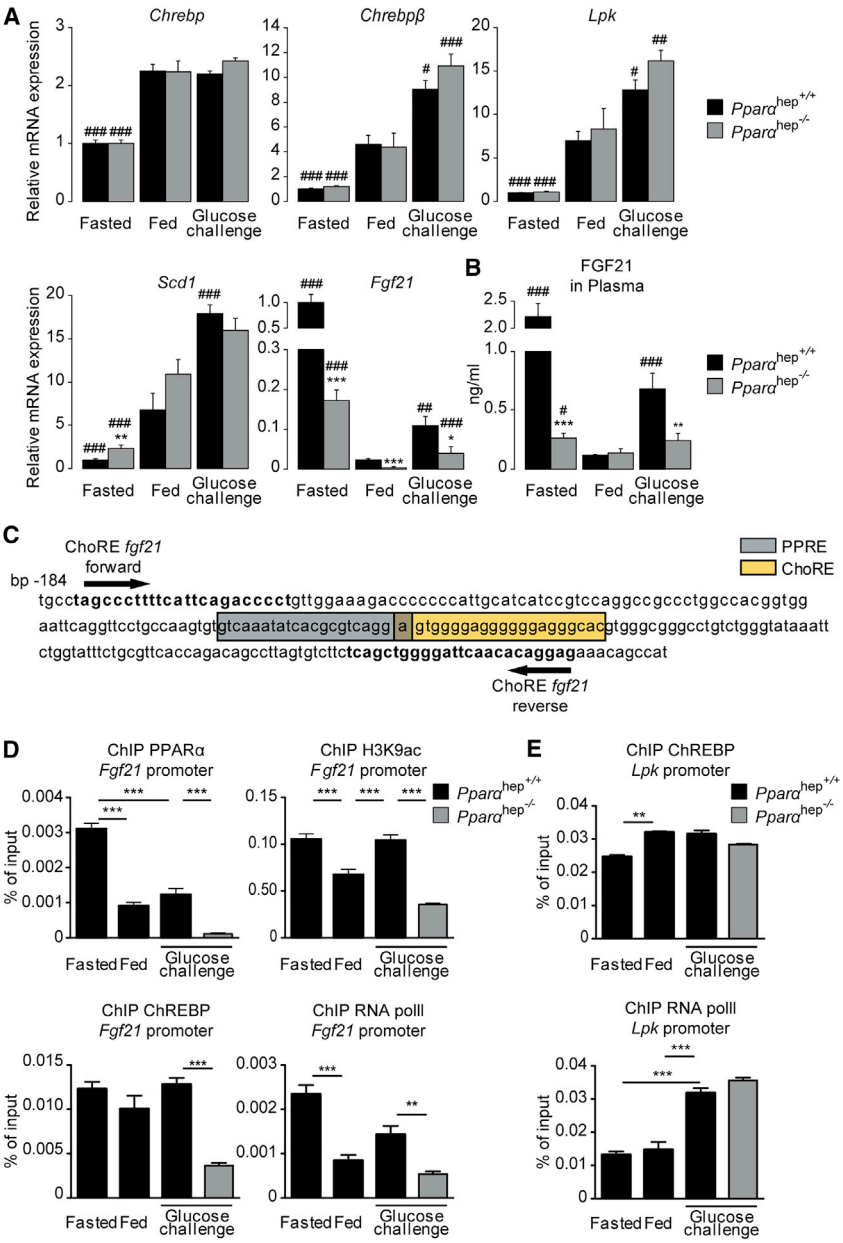

Figure 5. PPARα Is Required for the Glucose-Dependent Expression and Secretion of FGF21 by the Liver

Male $Ppar\alpha^{hep+/+}$ or $Ppar\alpha^{hep-/-}$ mice were assigned one of three treatment groups: (1) fasted 24 hr with free access to drinking water (fasted), (2) fed ad libitum with free access to drinking water (fed), or (3) fed ad libitum with access to a 20% glucose drinking water solution for 24 hr (glucose challenge).

(A) Relative gene expression of *Chrebp*, *Chrebpβ*, *Lpk*, *Scd1*, and *Fgf21* was determined by qPCR. Data are expressed as means ± SEM (n = 6 individual mice per group). Significance is based on two-way ANOVA followed by Bonferroni post hoc test (fasting or glucose versus fed; #p ≤ 0.05; ##p ≤ 0.01; ###p ≤ 0.001). Significance of the effect of genotype is based two-way ANOVA followed by Bonferroni post hoc test ($Ppar\alpha^{hep-/-}$ versus $Ppar\alpha^{hep+/+}$; *p ≤ 0.05; **p ≤ 0.01; ***p ≤ 0.001).

(B) ELISA quantification of FGF21 in plasma. Data are expressed as means ± SEM from n = 6 individual mice per group. Significance of the effect of fasting or glucose challenge is based on two-way ANOVA followed by post hoc test (fasting or glucose versus fed; #p ≤ 0.05; ##p ≤ 0.01; ###p ≤ 0.001). Significance of the effect of genotype is based on two-way ANOVA followed by Bonferroni post hoc test ($Ppar\alpha^{hep-/-}$ versus $Ppar\alpha^{hep+/+}$; *p ≤ 0.05; **p ≤ 0.01; ***p ≤ 0.001).

(C) *Fgf21* promoter sequence from the transcription start site to −184 bp. The PPARα binding site (PPRE) is indicated in gray. The ChREBP binding site (ChoRE) is indicated in yellow. Primers used for ChIP analysis are indicated on the sequence.

(D) ChIP analysis followed by qPCR of whole mouse liver tissue. Immunoprecipitation (IP) was conducted with PPARα, ChREBP, H3K9ac, and RNA Pol II antibodies. The DNA region of the *Fgf21* promoter was amplified using the primers indicated in (C).

(E) ChIP analysis followed by qPCR of whole mouse liver tissue. IP were conducted with ChREBP and RNA Pol II antibodies. Data are expressed as means ± SEM from n = 3 individual mice per group. Significance is based on two-way ANOVA followed by Bonferroni post hoc test (**p ≤ 0.01; ***p ≤ 0.001).

suggest that *Fgf21* promoter accessibility at the ChoRE is altered in the absence of PPARα by a mechanism that may partly rely on histone acetylation. To determine whether the potentiating effect of the HDAC inhibitor on glucose-induced *Fgf21* expression was due to enhanced ChREBP activity, experiments were performed in $Chrebp^{+/+}$ and $Chrebp^{-/-}$ hepatocytes (Figure 6C). Similar to what was observed in $Ppar\alpha^{hep+/+}$ hepatocytes (Figure 6B), the effect of glucose (25 mM) on *Fgf21* expression was increased when $Chrebp^{+/+}$ hepatocytes were treated with the HDAC inhibitor (Figure 6C). *Chrebp*, *Chrebpβ*, and *Lpk* followed a similar trend, with a significant effect observed for *Chrebp* (Figure 6C). Importantly, the potentiated effect of the HDAC inhibitor on *Fgf21* expression was lost in $Chrebp^{-/-}$ hepatocytes (Figure 6C), indicating a dependence on ChREBP activity. Altogether, our results suggest that PPARα is essential to allow ChREBP to gain access to the promoter of *Fgf21*. Moreover, our data show that the use of HDAC inhibitors enhances the ChREBP-dependent effect of glucose on *Fgf21* but cannot fully rescue the effect of PPARα deficiency.

Sucrose Intake Is Increased in Mice Lacking PPARα in the Liver

Finally, we determined whether the decrease in circulating FGF21 observed in glucose-challenged $Ppar\alpha^{hep-/-}$ mice (Figure 5B) paralleled with an increase in sucrose preference, since it was recently demonstrated that FGF21's action on the paraventricular nucleus of the hypothalamus blocks sugar-seeking behavior and sugar intake in mice (Talukdar et al., 2016; von Holstein-Rathlou et al., 2016). First, we observed

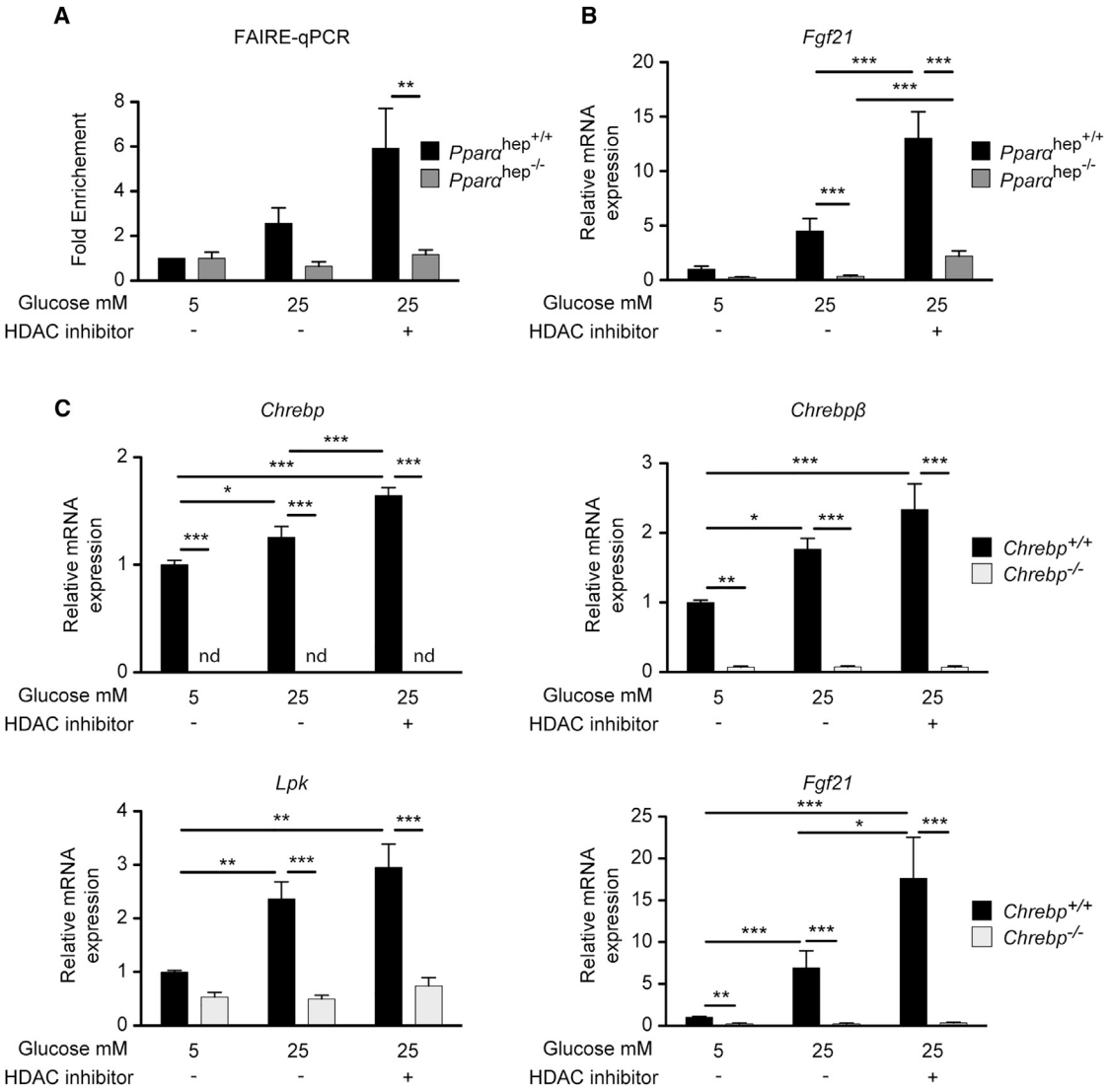

Figure 6. *Fgf21* Promoter Accessibility Is Reduced in the Absence of PPARα

(A and B) Primary hepatocytes derived from adult *Pparα*$^{hep+/+}$ or *Pparα*$^{hep-/-}$ mice were treated with 10 μM of the HADC inhibitor LBH589 or DMSO as a control for 24 hr in the presence of 5 or 25 mM glucose. (A) FAIRE-qPCR was performed as described in Experimental Procedures. (B) Fgf21 gene expression determined by qPCR. Data are presented as means ± SEM from 4 independent cultures performed in duplicate. Significance is based on two-way ANOVA followed by Bonferroni post hoc test (*p % 0.05; **p % 0.01; ***p % 0.001).

(C) Primary hepatocyte derived from adult *Chrebp*$^{+/+}$ or *Chrebp*$^{-/-}$ mice were treated with 10 μM of the HADC inhibitor LBH589 or with DMSO as control for 24 hr in the presence of medium containing 5 or 25 mM glucose. Relative gene expression of *Chrebp*, *Chrebpβ*, *Lpk*, and *Fgf21* was determined by qPCR.

Data are presented as means ± SEM from 4 independent cultures performed in duplicate. Significance is based on two-way ANOVA followed by Bonferroni post hoc test (*p ≤ 0.05; **p ≤ 0.01; ***p ≤ 0.001).

that there was no change in body weight or food or water intake in *Pparα* $^{hep-/-}$ compared to *Pparα* $^{hep+/+}$ mice fed with standard chow (Figures 7A–7C). Sucrose preference was then evaluated by giving *Pparα* $^{hep+/+}$ and *Pparα* $^{hep+/+}$ littermates matched for age and body weight free choice between a bottle containing a 10% sucrose solution and water (Figure 7D). Consumption, which was measured daily for 3 days, demonstrated that *Pparα* $^{hep-/-}$ mice consumed 30% more sucrose solution than *Pparα* $^{hep+/+}$ mice, while the volume of water drunk remained similar between genotypes (Figure 7E).

DISCUSSION

The regulation of FGF21 in the liver is complex due to the paradoxical regulation of this key hepatokine by fasting and glucose signals. In the current study, we uncovered a cross-talk between ChREBP and PPARα for the induction of hepatic FGF21 in response to a glucose challenge. The main finding of our study is that hepatic PPARα is necessary for the glucose-mediated induction of *Fgf21* by ChREBP.

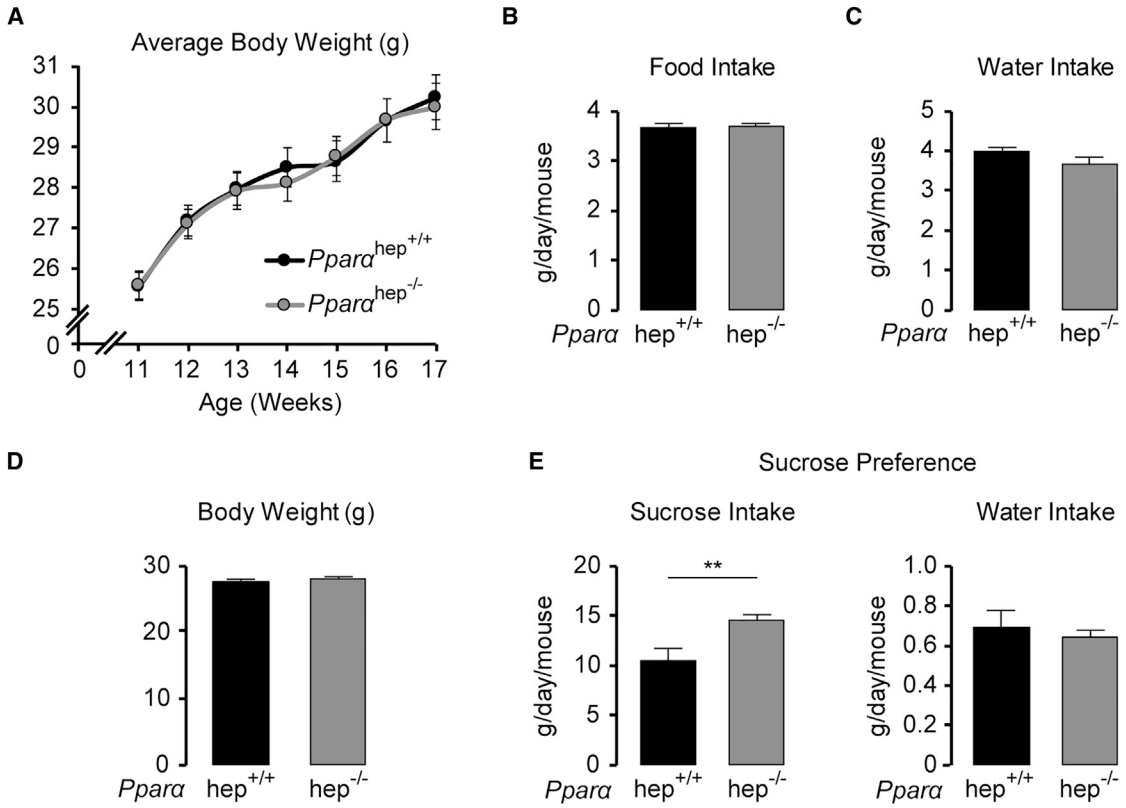

Figure 7. Sucrose Intake Is Increased in *Pparα*$^{hep-/-}$ Mice

(A–C) Average body weight gain (A), food (B) and water (C) intake of age-matched *Pparα*$^{hep+/+}$ and *Pparα*$^{hep-/-}$ mice (n = 12/group) over 6 weeks.
(D) Average body weight of age-matched male *Pparα*$^{hep+/+}$ and *Pparα*$^{hep-/-}$ mice used for the sucrose preference test (n = 16/group).
(E) *Pparα*$^{hep+/+}$ and *Pparα*$^{hep-/-}$ mice were given a 4-day adaptation period with two water bottles. A 10% sucrose solution was added to one of the water bottles for 3 days following adaptation and intake of sucrose solution and water was recorded daily for 3 days. Data are presented as means ± SEM from 5 to 6 individual mice. Significance is based on 2-way ANOVA followed by Bonferroni post hoc test (**$p \leq 0.01$).

Key to β-oxidation and ketogenesis, FGF21 mobilizes energy in the liver for peripheral use, protecting against dyslipidemia and hepatosteatosis (Inagaki et al., 2007; Potthoff et al., 2009). First described as a fasting hormone regulated by PPARα, transcriptional regulation of *Fgf21* in the context of excessive blood glucose has only recently been explored (Talukdar et al., 2016; von Holstein-Rathlou et al., 2016), despite early identification of the glucose-sensing region, ChoRE, on the *Fgf21* promoter in both mouse (−74 to −52 bp) and human (−380 to −366 bp) (Iizuka et al., 2009). Our experiments confirm that FGF21 is significantly expressed and released by cultured mouse and human hepatocytes in response to glucose upon ChREBP binding to the ChoRE (Iizuka et al., 2009; Uebanso et al., 2011). Our study demonstrates that deletion of ChREBP blunts transcription and secretion of hepatic FGF21 in response to glucose. Importantly, hepatic rescue of ChREBP in global ChREBP knockout mice is sufficient to restore *Fgf21* mRNA in the liver and protein in circulation, demonstrating the specificity of hepatic ChREBP activity on the induction of FGF21 in response to a glucose challenge. Interestingly, ChREBP rescue in the liver of *Chrebp*$^{-/-}$ mice significantly normalized blood glucose concentrations to control levels. This suggests that hepatic ChREBP activity and not peripheral ChREBP is essential for glucose-homeostasis maintenance. This result is consistent with a previous study in which hepatic ChREBP overexpression improved impaired glucose tolerance of high-fat-diet-challenged mice (Benhamed et al., 2012) and is in agreement with a recent study reporting that liver *Chrebp* knockout mice exhibit impaired insulin sensitivity and glucose intolerance (Jois et al., 2017). In this study, while hepatic *Chrebp* deletion protected against hepatic steatosis, it also resulted in gene expression changes in white and brown adipose tissues, suggesting inter-organ communication. The contribution of ChREBP to whole-body energy balance may therefore rely on its regulation of lipid species and/or hepatokine production that could contribute to inter-tissue coordination of energy homeostasis.

Activated in response to free fatty acids liberated from adipocytes during fasting (Montagner et al., 2016), a role for hepatocyte PPARα in the response to glucose had not yet been identified. Our study reveals that the synergic induction of *Fgf21* by glucose and the PPARα agonist Wy-14643 occurs in both mouse and human hepatocytes. We hypothesize that this cross-talk is specific to *Fgf21*, as we found no effect of glucose

on other typical PPARα target genes. This *Fgf21* specificity may be due to the proximity of ChREBP- and PPARα-binding sites on the *Fgf21* proximal promoter, as both a PPRE and a ChoRE region coexist (−88 to −54 bp) (Girer et al., 2016). Microarray analysis comparing gene regulation during fasting and glucose challenge highlights a small subset of genes that are upregulated in both conditions. Of those genes *Fgf21* is the most significantly induced. Therefore, FGF21 is a unique hepatic hormone showing dual regulation by fasting and carbohydrate signaling. Few publications have proposed a dialog between ChREBP and PPARs for the coordination of energy metabolism. Some examples of cross-talk and regulatory mechanisms have been described for lipid metabolism in brown adipose (Iizuka et al., 2013) and pancreatic β cell function (Boergesen et al., 2011). In the liver, it was also described that the PPARα co-factor PPAR γ coactivator-1β (PGC-1β) can act as a co-activator of ChREBP in response to glucose. PGC-1β is known to activate genes responsible for fatty acid oxidation and hepatic gluconeogenesis during fasting (Vega et al., 2000; Yoon et al., 2001), and it was also reported to upregulate de novo lipogenic genes during glucose stimulation in a ChREBP-dependent manner (Chambers et al., 2013). Altogether, these studies strongly suggest a direct and/or indirect interaction between ChREBP and the PPAR nuclear receptor family.

Here, we reveal a ChREBP-PPARα dialog in hepatocytes required for the induction of *Fgf21* by glucose. Indeed, despite normal hepatic ChREBP activity toward glycolytic and lipogenic genes, we report that in the absence of PPARα, ChREBP binding to the *Fgf21* ChoRE is significantly reduced, suggesting that hepatocyte PPARα is necessary for the ChREBP-mediated induction of *Fgf21* in response to glucose. Our study also reports that *Fgf21* promoter accessibility is reduced in the absence of PPARα. Deficient recruitment of ChREBP as well as Pol II was observed at the proximal *Fgf21* promoter locus under elevated glucose conditions in the liver of mice lacking hepatocyte PPARα. The fact that epigenetic marks (i.e., H3K9ac) of active transcription were reduced at the *Fgf21* promoter when PPARα was lacking in liver, under both fasting and glucose conditions, also supports the hypothesis of reduced promoter accessibility. Indeed, even under conditions of ChREBP overexpression, *Fgf21* expression was not efficiently induced in the context of PPARα deficiency. Further experiments will be needed to determine whether PPARα acts as a "pioneer" transcription factor for *Fgf21* transcription. Among several described functions, pioneer factors can trigger the opening and/or organization of the local chromatin, in turn allowing the binding of other transcription factors, histone-modification enzymes, chromatin modifiers, and/or nucleosome remodelers (Zaret and Carroll, 2011). Of note, an HDAC inhibitor potentiated a ChREBP-dependent effect of glucose on *Fgf21* expression in primary hepatocytes. The HDAC inhibitor strategy in glucose-challenged PPARα-deficient hepatocytes only led to a modest restoration of *FgF21* expression. While this approach was not sufficient to fully restore accessibility to the *Fgf21* promoter, it does suggest that *Fgf21* promoter accessibility at the ChoRE is altered in the absence of PPARα by a mechanism that may partly rely on histone acetylation. We employed FAIRE-qPCR analysis to determine *Fgf21* promoter accessibility in response to glucose. A more sensitive approach, the assay for transposase-accessible chromatin with high-throughput sequencing (ATAC-seq) (Buenrostro et al., 2013) may have allowed us to determine whether *Fgf21* promoter accessibility is indeed modified by an HDAC inhibitor strategy in $Ppar\alpha^{hep-/-}$ hepatocytes. While other molecular mechanisms are clearly involved, the implication of specific HDACs should be further investigated, since it was recently shown that PPARα prevents the recruitment of HDAC3 to the *Fgf21* promoter in hepatocytes when concentrations of β-hydroxybutyrate, a key product of β-oxidation, are elevated (Rando et al., 2016).

At the physiological level, we observed that $Ppar\alpha^{hep-/-}$ mice consumed more sucrose (+30%) than $Ppar\alpha^{hep+/+}$ mice. Two studies have recently unraveled the mechanistic link between sucrose-derived FGF21 and nutrient preference (Talukdar et al., 2016; von Holstein-Rathlou et al., 2016). FGF21 production in response to carbohydrates was shown to markedly reduce sweet taste preference and suppress consumption of simple sugars by acting on specific regions of the brain (Talukdar et al., 2016; von Holstein-Rathlou et al., 2016). In these studies, hepatic FGF21 production in response to carbohydrate intake was attributed to ChREBP activity. The fact that PPARα is also involved in this liver-to-brain axis following simple sugar consumption opens new molecular path of regulation of macronutrient preference/intake and expands liver PPARα function from a fasting regulator to a modulator affecting the physiological sugar response.

In conclusion, we identify a transcriptional node in the control of hepatic FGF21 in response to glucose. The glucose sensor ChREBP requires PPARα for the induction of FGF21 in response to dietary sugar. This is a unique collaboration between transcription factors that are activated in response to distinct nutritional conditions (high glucose for ChREBP and fasting for PPARα). These data imply that drug targeting of PPARα may exert part of its beneficial effects on metabolic homeostasis by supporting the ChREBP-induced loop controlling sweet preference via FGF21.

EXPERIMENTAL PROCEDURES

Generation of ChREBP Knockout Mice

Mice lacking exons 9–15 of the *Chrebp* gene were generated through homologous recombination. Correspondence regarding $Chrebp^{-/-}$ mice should be addressed to R.D. (renaud.dentin@inserm.fr) and C.P. (catherine.postic@inserm.fr). Experimental details are provided in Supplemental Experimental Procedures.

Animals

10- to 12-week-old adult male C57BL/6J, $Chrebp^{+/+}$, $Chrebp^{-/-}$, $Ppar\alpha^{hep+/+}$, and $Ppar\alpha^{hep-/-}$ mice (Montagner et al., 2016) were used for all in vivo experiments. For hepatocyte cultures, male and female mice were used as described in the figure legends. Procedures were carried out according to the French guidelines for the care and use of experimental animals (animal authorization agreement number CEEA34.AFB/CP.082.12, Paris Descartes Ethical Committee). Mice were maintained in a 12-hr light/dark cycle with water and a standard diet (65% carbohydrate, 11% fat, and 24% protein) unless otherwise specified. Nutritional challenges details are described in Supplemental Experimental Procedures.

Injection of Adenovirus In Vivo

Adenovirus coding GFP and $ChREBP^{CA}$ (ChREBP isoform deleted of the LID domain) (Li et al., 2006) produced by Laboratoire de thérapie génique (Nantes, France; requests to R.D. at renaud.dentin@inserm.fr) were delivered through

penis vein injection (3×10^9 [pfu]/mouse) to adult mice. Four days later, nutritional protocols were applied.

Primary Cultures of Human and Mouse Hepatocytes

Human hepatocytes were prepared from lobectomy segments resected from adult patients under the approval of the National Ethics Committee as described previously (Pichard et al., 2006; Marmier et al., 2015). Mouse hepatocytes were isolated as described previously (Dentin et al., 2004). Experimental details regarding culture conditions are provided in the figure legends and Supplemental Experimental Procedures.

ChIP Analysis

In vivo chromatin immunoprecipitation (ChIP) assays from mouse livers were performed by Active Motif. Briefly, genomic DNA regions of interest were isolated using antibodies against H3K9Ac (Active Motif), RNA Pol II (Active Motif), ChREBP (Novus), and PPARα (Santa Cruz Biotechnology). qPCR reactions were carried out in triplicate using SYBR Green Supermix (Bio-Rad) on a CFX Connect Real Time PCR system. Positive and negative control sites were tested for each factor as well as the sites of interest. The resulting signals were normalized for primer efficiency by carrying out qPCR for each primer pair using input DNA (pooled unprecipitated genomic DNA from each sample). Specific enrichment was expressed as percentage of input. Further details are provided in Supplemental Experimental Procedures.

In vitro ChIP assays from cultured hepatocytes were performed as described previously (Marmier et al., 2015). Briefly, genomic DNA regions of interest were isolated using antibodies against ChREBP (Novus) and immunoglobulin G (IgG) (Cell Signaling). DNA fragments were quantified by qPCR using primers described in Table S1. Results are expressed as fold enrichment. Further details are provided in Supplemental Experimental Procedures.

FAIRE-qPCR

FAIRE-qPCR was performed in $Ppar\alpha^{hep+/+}$ and $Ppar\alpha^{hep-/-}$ hepatocytes using a protocol previously described (Simon et al., 2012). Briefly, cells were treated with 1% formaldehyde at room temperature for 5 min to form DNA-protein crosslinks, and the crosslinking was stopped by addition of glycine to a final concentration of 125 mM. FAIRE was analyzed by qPCR on genomic DNA using the ChoRE *Fgf21* primers (Figure 5C) and calculated using relative enrichment for each amplicon using the comparative Ct method, such that a ratio is calculated for the signal from the FAIRE sample relative to the input control DNA signal. Results are expressed as fold enrichment. Experimental details are provided in Supplemental Experimental Procedures.

Gene Expression Analysis

Total cellular RNA was extracted using the SV total RNA isolation system (Promega). For qPCR analysis, total RNA samples (2 μg) were reverse transcribed using the High Capacity cDNA Reverse Transcription Kit (Applied Biosystems). Primers for SYBR green assays are presented in Tables S2 and S3. Primers used to measure *Chrebp* expression were designed to detect the *Chrebpα* and *Chrebpβ* isoforms. A specific primer to detect only the β isoform was also used. Primers for *Vnn1*, *Cyp4a10*, and *Cyp4a14* were previously described (Montagner et al., 2016). Amplifications were performed on an ABI Prism 7300 Real Time PCR System (Applied Biosystems). qPCR data were normalized by TATA-box binding protein (TBP) mRNA levels or 18S ribosomal (18S) for human samples and analyzed with LinRegPCR.22.

Transcriptomic profiles were obtained using Agilent SurePrint G3 Mouse V2 GE 8x60K (Design 074809) following the manufacturer's instructions. Data were analyzed with R (http://www.r-project.org) using Bioconductor packages (http://www.bioconductor.org, v 2.12; Gentleman et al., 2004) as described in GEO: GSE26728. A model was fitted using the limma lmFit function (Wettenhall and Smyth, 2004). Correction for multiple testing was applied using a false discovery rate (Benjamini and Hochberg, 1995). Probes with adjusted $p \leq 0.05$ were considered differentially expressed (n = 6). Hierarchical clustering was applied and the differentially expressed probes using 1 − Pearson correlation coefficient as distance and Ward's criterion for agglomeration. The resulting dendrogram were illustrated as a heatmap. The enrichment of gene ontology (GO) biological processes was evaluated using a conditional hypergeometric test (GOstats package; Falcon and Gentleman, 2007).

Western Blotting Analysis

Proteins from hepatocytes and liver tissue were extracted from whole-cell lysates. Proteins were subjected to 10% SDS-PAGE gels and transferred to nitrocellulose membranes. Rabbit polyclonal ChREBP (1:1,000, Novus Biologicals) and L-PK (1:1,500, a gift from Dr. Axel Kahn) antibodies were used. Protein β-actin (1:5,000) (Cell Signaling Technology) was used to normalize data.

Analytical Analysis

Blood glucose was measured from total blood using an Accu-Check glucometer (Roche). Liver triglycerides were measured with a colorimetric diagnostic kit (Triglycerides FS, Diasys). Serum insulin concentrations were determined using a rat insulin ELISA assay kit (Crystal Chem) with a mouse insulin standard. The mouse ELISA kit (Millipore) was used to measure FGF21 in cell culture medium (30 μL of medium was used) and mouse plasma (20 μL).

Statistical Analysis

Data represent at least three independent experiments, are reported as means ± SEM, and were analyzed with analysis of variance using Prism 5.0 (GraphPad) software. A Student's t test was used when comparing two groups (followed by Mann-Whitney post hoc test) or two-way ANOVA when comparing three or more groups followed by a Bonferroni post hoc test. Statistical significance was defined as $p < 0.05$.

DATA AND SOFTWARE AVAILABILITY

The accession number for the microarray data reported in this paper is GEO: GSE92502.

SUPPLEMENTAL INFORMATION

Supplemental Information includes Supplemental Experimental Procedures, five figures, and three tables and can be found with this article online at https://doi.org/10.1016/j.celrep.2017.09.065.

AUTHOR CONTRIBUTIONS

A.I., A.M., F.B., C.P., and H.G. designed and performed experiments, analyzed the data, and wrote the manuscript. A.M., A.P., F.B., E.A., C.P., and H.G. revised the manuscript. E.A., A.P., E.F., M.R., C.L., V.F., S.M., and M.C. performed experiments and analyzed the data. E.T., M. Do-Cruzeiro, F.L., R.D., and C.P. generated ChREBP knockout mice. M. Daujat-Chavanieu and S.G.-C. provided human hepatocytes. Y.L. performed microarray analysis and biostatics analysis. R.D., S.G., A.-F.B., J.G., and W.W. provided critical reagents and comments.

ACKNOWLEDGMENTS

We would like to thank Dr. B. Staels and Dr. P. Lefebvre (Inserm U1011, Lille), Dr. N. Venteclef (Inserm UMR_S1138, Paris), and Dr. D. Langin (Inserm UMR 1048, Toulouse) for scientific discussion. We also thank Dr. A. Kayali and Dr. T. Issad (Institut Cochin, Inserm U1016) for critical reading of the manuscript. We thank L. Francese, S. Topçu (Institut Cochin, Inserm U1016), C. Naylies (GeT-TRiX, INRA ToxAlim), and G.Michel for providing excellent technical assistance. We thank the animal facility staff (EZOP, INRA ToxAlim) for their excellent work. H. Guillou's lab (TIM, ToxAlim) is supported by grants from Région Occitanie. W.W. was supported by a start-up grant from Lee Kong Chian School of Medicine, Nanyang Technological University. C. Postic's lab (U1016-Institut Cochin) is supported by grants from ChroME Network (Marie Curie Sklodowska Action H2020-MSCA-ITN-2015-675610), the Foundation for the Medical Research (FRM) (DEQ20150331744), and the European Foundation for the Study of Diabetes (EFSD) Novonordisk. H. Guillou's and C. Postic's labs are also supported by grants from the National Agency for Research (ANR) (ANR-12BSV1-0025-ObeLiP and ANR-15-CE14-0026-Hepatokind). R. Dentin's lab (U1016-Institut Cochin) is supported by the European Research

Council (ERC-2013-StG-336629) and the city of Paris (Projet Emergences-2011). This project is performed in the context of the DHU authors (autoimmune and hormonal diseases).

Received: December 20, 2016
Revised: August 15, 2017
Accepted: September 20, 2017
Published: October 10, 2017

REFERENCES

Abdul-Wahed, A., Guilmeau, S., and Postic, C. (2017). Sweet sixteenth for ChREBP: established roles and future goals. Cell Metab. *26*, 324–341.

Badman, M.K., Pissios, P., Kennedy, A.R., Koukos, G., Flier, J.S., and Maratos-Flier, E. (2007). Hepatic fibroblast growth factor 21 is regulated by PPARalpha and is a key mediator of hepatic lipid metabolism in ketotic states. Cell Metab. *5*, 426–437.

Benhamed, F., Denechaud, P.-D., Lemoine, M., Robichon, C., Moldes, M., Bertrand-Michel, J., Ratziu, V., Serfaty, L., Housset, C., Capeau, J., et al. (2012). The lipogenic transcription factor ChREBP dissociates hepatic steatosis from insulin resistance in mice and humans. J. Clin. Invest. *122*, 2176–2194.

Benjamini, Y., and Hochberg, Y. (1995). Controlling the false discovery rate: A practical and powerful approach to multiple testing. Journal of the Royal Statistical Society. Series B (Methodological) *57*, 289–300.

Berglund, E.D., Li, C.Y., Bina, H.A., Lynes, S.E., Michael, M.D., Shanafelt, A.B., Kharitonenkov, A., and Wasserman, D.H. (2009). Fibroblast growth factor 21 controls glycemia via regulation of hepatic glucose flux and insulin sensitivity. Endocrinology *150*, 4084–4093.

Boergesen, M., Poulsen, LI., Schmidt, S.F., Frigerio, F., Maechler, P., and Mandrup, S. (2011). ChREBP mediates glucose repression of peroxisome proliferator-activated receptor alpha expression in pancreatic beta-cells. J. Biol. Chem. *286*, 13214–13225.

Buenrostro, J.D., Giresi, P.G., Zaba, L.C., Chang, H.Y., and Greenleaf, W.J. (2013). Transposition of native chromatin for multimodal regulatory analysis and personal epigenomics. Nat. Methods *10*, 1213–1218.

Chambers, K.T., Chen, Z., Lai, L., Leone, T.C., Towle, H.C., Kralli, A., Crawford, P.A., and Finck, B.N. (2013). PGC-1β and ChREBP partner to cooperatively regulate hepatic lipogenesis in a glucose concentration-dependent manner. Mol. Metab. *2*, 194–204.

Christodoulides, C., Dyson, P., Sprecher, D., Tsintzas, K., and Karpe, F. (2009). Circulating fibroblast growth factor 21 is induced by peroxisome proliferator-activated receptor agonists but not ketosis in man. J. Clin. Endocrinol. Metab. *94*, 3594–3601.

Coskun, T., Bina, H.A., Schneider, M.A., Dunbar, J.D., Hu, C.C., Chen, Y., Moller, D.E., and Kharitonenkov, A. (2008). Fibroblast growth factor 21 corrects obesity in mice. Endocrinology *149*, 6018–6027.

Dentin, R., Pégorier, J.P., Benhamed, F., Foufelle, F., Ferré, P., Fauveau, V., Magnuson, M.A., Girard, J., and Postic, C. (2004). Hepatic glucokinase is required for the synergistic action of ChREBP and SREBP-1c on glycolytic and lipogenic gene expression. J. Biol. Chem. *279*, 20314–20326.

Falcon, S., and Gentleman, R. (2007). Using GOstats to test gene lists for GO term association. Bioinformatics *23*, 257–258.

Fisher, F.M., Estall, J.L., Adams, A.C., Antonellis, P.J., Bina, H.A., Flier, J.S., Kharitonenkov, A., Spiegelman, B.M., and Maratos-Flier, E. (2011). Integrated regulation of hepatic metabolism by fibroblast growth factor 21 (FGF21) in vivo. Endocrinology *152*, 2996–3004.

Gälman, C., Lundåsen, T., Kharitonenkov, A., Bina, H.A., Eriksson, M., Hafström, I., Dahlin, M., Amark, P., Angelin, B., and Rudling, M. (2008). The circulating metabolic regulator FGF21 is induced by prolonged fasting and PPARalpha activation in man. Cell Metab. *8*, 169–174.

Gentleman, R.C., Carey, V.J., Bates, D.M., Bolstad, B., Dettling, M., Dudoit, S., Ellis, B., Gautier, L., Ge, Y., Gentry, J., et al. (2004). Bioconductor: open software development for computational biology and bioinformatics. Genome Biol. *5*, R80.

Girer, N.G., Murray, I.A., Omiecinski, C.J., and Perdew, G.H. (2016). Hepatic aryl hydrocarbon receptor attenuates fibroblast growth factor 21 expression. J. Biol. Chem. *291*, 15378–15387.

Goldstein, I., and Hager, G.L. (2015). Transcriptional and chromatin regulation during fasting: the genomic era. Trends Endocrinol. Metab. *26*, 699–710.

Herman, M.A., Peroni, O.D., Villoria, J., Schön, M.R., Abumrad, N.A., Blüher, M., Klein, S., and Kahn, B.B. (2012). A novel ChREBP isoform in adipose tissue regulates systemic glucose metabolism. Nature *484*, 333–338.

Iizuka, K., Takeda, J., and Horikawa, Y. (2009). Glucose induces FGF21 mRNA expression through ChREBP activation in rat hepatocytes. FEBS Lett. *583*, 2882–2886.

Iizuka, K., Wu, W., Horikawa, Y., Saito, M., and Takeda, J. (2013). Feedback looping between ChREBP and PPARα in the regulation of lipid metabolism in brown adipose tissues. Endocr. J. *60*, 1145–1153.

Imai, Y., Ohta, E., Takeda, S., Sunamura, S., Ishibashi, M., Tamura, H., Wang, Y.H., Deguchi, A., Tanaka, J., Maru, Y., and Motoji, T. (2016). Histone deacetylase inhibitor panobinostat induces calcineurin degradation in multiple myeloma. JCI Insight *1*, e85061.

Inagaki, T., Dutchak, P., Zhao, G., Ding, X., Gautron, L., Parameswara, V., Li, Y., Goetz, R., Mohammadi, M., Esser, V., et al. (2007). Endocrine regulation of the fasting response by PPARalpha-mediated induction of fibroblast growth factor 21. Cell Metab. *5*, 415–425.

Iroz, A., Couty, J.P., and Postic, C. (2015). Hepatokines: unlocking the multi-organ network in metabolic diseases. Diabetologia *58*, 1699–1703.

Jaeger, D., Schoiswohl, G., Hofer, P., Schreiber, R., Schweiger, M., Eichmann, T.O., Pollak, N.M., Poecher, N., Grabner, G.F., Zierler, K.A., et al. (2015). Fasting-induced G0/G1 switch gene 2 and FGF21 expression in the liver are under regulation of adipose tissue derived fatty acids. J. Hepatol. *63*, 437–445.

Jois, T., Chen, C., Howard, V., Harvey, R., Youngs, K., Thalmann, C., Saha, P., Chan, L., Cowley, M.A., and Sleeman, M.W. (2017). Deletion of hepatic carbohydrate response element binding protein (ChREBP) impairs glucose homeostasis and hepatic insulin sensitivity in mice. Mol. Metab. Published online July 18, 2017. https://doi.org/10.1016/j.molmet.2017.07.006.

Kawaguchi, T., Takenoshita, M., Kabashima, T., and Uyeda, K. (2001). Glucose and cAMP regulate the L-type pyruvate kinase gene by phosphorylation/dephosphorylation of the carbohydrate response element binding protein. Proc. Natl. Acad. Sci. USA *98*, 13710–13715.

Kersten, S., Seydoux, J., Peters, J.M., Gonzalez, F.J., Desvergne, B., and Wahli, W. (1999). Peroxisome proliferator-activated receptor alpha mediates the adaptive response to fasting. J. Clin. Invest. *103*, 1489–1498.

Kharitonenkov, A., and Adams, A.C. (2013). Inventing new medicines: The FGF21 story. Mol. Metab. *3*, 221–229.

Kharitonenkov, A., Wroblewski, V.J., Koester, A., Chen, Y.F., Clutinger, C.K., Tigno, X.T., Hansen, B.C., Shanafelt, A.B., and Etgen, G.J. (2007). The metabolic state of diabetic monkeys is regulated by fibroblast growth factor-21. Endocrinology *148*, 774–781.

Kroetz, D.L., Yook, P., Costet, P., Bianchi, P., and Pineau, T. (1998). Peroxisome proliferator-activated receptor alpha controls the hepatic CYP4A induction adaptive response to starvation and diabetes. J. Biol. Chem. *273*, 31581–31589.

Leone, T.C., Weinheimer, C.J., and Kelly, D.P. (1999). A critical role for the peroxisome proliferator-activated receptor alpha (PPARalpha) in the cellular fasting response: the PPARalpha-null mouse as a model of fatty acid oxidation disorders. Proc. Natl. Acad. Sci. USA *96*, 7473–7478.

Li, M.V., Chang, B., Imamura, M., Poungvarin, N., and Chan, L. (2006). Glucose-dependent transcriptional regulation by an evolutionarily conserved glucose-sensing module. Diabetes *55*, 1179–1189.

Lundåsen, T., Hunt, M.C., Nilsson, L.-M., Sanyal, S., Angelin, B., Alexson, S.E.H., and Rudling, M. (2007). PPARalpha is a key regulator of hepatic FGF21. Biochem. Biophys. Res. Commun. *360*, 437–440.

Markan, K.R., Naber, M.C., Ameka, M.K., Anderegg, M.D., Mangelsdorf, D.J., Kliewer, S.A., Mohammadi, M., and Potthoff, M.J. (2014). Circulating FGF21 is liver derived and enhances glucose uptake during refeeding and overfeeding. Diabetes *63*, 4057–4063.

Marmier, S., Dentin, R., Daujat-Chavanieu, M., Guillou, H., Bertrand-Michel, J., Gerbal-Chaloin, S., Girard, J., Lotersztajn, S., and Postic, C. (2015). Novel role for carbohydrate responsive element binding protein in the control of ethanol metabolism and susceptibility to binge drinking. Hepatology *62*, 1086–1100.

Montagner, A., Polizzi, A., Fouché, E., Ducheix, S., Lippi, Y., Lasserre, F., Barquissau, V., Régnier, M., Lukowicz, C., Benhamed, F., et al. (2016). Liver PPARα is crucial for whole-body fatty acid homeostasis and is protective against NAFLD. Gut *65*, 1202–1214.

Ong, K.L., Rye, K.-A., O'Connell, R., Jenkins, A.J., Brown, C., Xu, A., Sullivan, D.R., Barter, P.J., and Keech, A.C.; FIELD study investigators (2012). Long-term fenofibrate therapy increases fibroblast growth factor 21 and retinol-binding protein 4 in subjects with type 2 diabetes. J. Clin. Endocrinol. Metab. *97*, 4701–4708.

Pichard, L., Raulet, E., Fabre, G., Ferrini, J.B., Ourlin, J.-C., and Maurel, P. (2006). Human hepatocyte culture. Methods Mol. Biol. *320*, 283–293.

Potthoff, M.J., Inagaki, T., Satapati, S., Ding, X., He, T., Goetz, R., Mohammadi, M., Finck, B.N., Mangelsdorf, D.J., Kliewer, S.A., and Burgess, S.C. (2009). FGF21 induces PGC-1alpha and regulates carbohydrate and fatty acid metabolism during the adaptive starvation response. Proc. Natl. Acad. Sci. USA *106*, 10853–10858.

Rando, G., Tan, C.K., Khaled, N., Montagner, A., Leuenberger, N., Bertrand-Michel, J., Paramalingam, E., Guillou, H., and Wahli, W. (2016). Glucocorticoid receptor-PPARα axis in fetal mouse liver prepares neonates for milk lipid catabolism. eLife *5*, e11853.

Sánchez, J., Palou, A., and Picó, C. (2009). Response to carbohydrate and fat refeeding in the expression of genes involved in nutrient partitioning and metabolism: striking effects on fibroblast growth factor-21 induction. Endocrinology *150*, 5341–5350.

Simon, J.M., Giresi, P.G., Davis, I.J., and Lieb, J.D. (2012). Using formaldehyde-assisted isolation of regulatory elements (FAIRE) to isolate active regulatory DNA. Nat. Protoc. *7*, 256–267.

Talukdar, S., Owen, B.M., Song, P., Hernandez, G., Zhang, Y., Zhou, Y., Scott, W.T., Paratala, B., Turner, T., Smith, A., et al. (2016). FGF21 Regulates Sweet and Alcohol Preference. Cell Metab. *23*, 344–349.

Uebanso, T., Taketani, Y., Yamamoto, H., Amo, K., Ominami, H., Arai, H., Takei, Y., Masuda, M., Tanimura, A., Harada, N., et al. (2011). Paradoxical regulation of human FGF21 by both fasting and feeding signals: is FGF21 a nutritional adaptation factor? PLoS ONE *6*, e22976.

Vega, R.B., Huss, J.M., and Kelly, D.P. (2000). The coactivator PGC-1 cooperates with peroxisome proliferator-activated receptor alpha in transcriptional control of nuclear genes encoding mitochondrial fatty acid oxidation enzymes. Mol. Cell. Biol. *20*, 1868–1876.

von Holstein-Rathlou, S., BonDurant, L.D., Peltekian, L., Naber, M.C., Yin, T.C., Claflin, K.E., Urizar, A.I., Madsen, A.N., Ratner, C., Holst, B., et al. (2016). FGF21 mediates endocrine control of simple sugar intake and sweet taste preference by the liver. Cell Metab. *23*, 335–343.

Wettenhall, J.M., and Smyth, G.K. (2004). limmaGUI: a graphical user interface for linear modeling of microarray data. Bioinformatics *20*, 3705–3706.

Yoon, J.C., Puigserver, P., Chen, G., Donovan, J., Wu, Z., Rhee, J., Adelmant, G., Stafford, J., Kahn, C.R., Granner, D.K., et al. (2001). Control of hepatic gluconeogenesis through the transcriptional coactivator PGC-1. Nature *413*, 131–138.

Zaret, K.S., and Carroll, J.S. (2011). Pioneer transcription factors: establishing competence for gene expression. Genes Dev. *25*, 2227–2241.

Cell Reports, Volume *21*

Supplemental Information

A Specific ChREBP and PPARα Cross-Talk Is Required for the Glucose-Mediated FGF21 Response

Alison Iroz, Alexandra Montagner, Fadila Benhamed, Françoise Levavasseur, Arnaud Polizzi, Elodie Anthony, Marion Régnier, Edwin Fouché, Céline Lukowicz, Michèle Cauzac, Emilie Tournier, Marcio Do-Cruzeiro, Martine Daujat-Chavanieu, Sabine Gerbal-Chalouin, Véronique Fauveau, Solenne Marmier, Anne-Françoise Burnol, Sandra Guilmeau, Yannick Lippi, Jean Girard, Walter Wahli, Renaud Dentin, Hervé Guillou, and Catherine Postic

Supplementary information

Generation of ChREBP knockout mice

Mice lacking exon 9 through 15 of the *Chrebp* gene were generated through homologous recombination (*Chrebp*$^{-/-}$ mice). Correspondence regarding *Chrebp*$^{-/-}$ mice should be addressed to renaud.dentin@inserm.fr and catherine.postic@inserm.fr. A vector containing the *Chrebp* sequence with the addition of two Lox-P sites flanking the coding exons 9-15 and a FRT-flanked hygromycin-resistant cassette was constructed (Figure S2). Clones were then selected after validation by 3 PCR sequences targeting i) 5' region homologue ii) 3' region homologue iii) floxed fragment. Homologous recombination of the target construct at the appropriate site was confirmed by Southern blot analysis followed by sequencing. Validated ES cells containing the target construct were injected in C57BL/6N derived blastocystes. Male agouti progeny were then bred with female C57BL/6J "flippase" mice to remove the hygromycin-resistant cassette. F1 progeny were crossed with *EllaCre* transgenic mice (Holzenberger et al. 2000) to ubiquitously remove the *loxP* floxed exons 9 to 15 from the *Chrebp* locus. This allowed generation of global *Chrebp*$^{-/-}$ mice (total excision of the *loxP*-flanked sequence) from a single germ-line mutation. Mice were genotyped using specific primers in Supplemental Table. S1. Loss of *Chrebp* expression was confirmed by qPCR and by western blot.

Nutritional challenges

All *in vivo* experiments were performed on adult (1à-12 week-old) male mice. All mice were sacrificed at ZT14 (14h after the start of light period in animal housing unit). Fasted mice were fasted starting at 11pm and sacrificed 24 hours later. Fasted and fed animals had free access to drinking water. Glucose treated mice were allowed ad libitum access to standard diet in addition to a 20% glucose solution (Sigma, G7021). To

measure sucrose intake, *Pparα*$^{hep+/+}$ and *Pparα*$^{hep-/-}$ mice (Montagner et al. 2016) were given free choice between a bottle containing a 10% sucrose solution or water. Consumption was measured daily during three days.

Culture conditions for primary mouse and human hepatocytes

For adenoviral infections, mouse hepatocytes from either female or male mice (as indicated in figure legens) were incubated under low glucose concentration (5 mM) with specific adenovirus (3 pfu/cell) for 24 h. For glucose stimulation experiments, hepatocytes were incubated with insulin (100 nM) in the presence of various glucose concentrations (5 to 30 mM) for 24 hours. For mannitol experiments, mouse hepatocytes were incubated with insulin (100 nM) in the presence of concentrations of mannitol (5 to 30 mM) for 24 hours. For HDAC inhibitor experiments, mouse hepatocytes were treated 10 μM of the HDAC inhibitor LBH589 (Panobinostat, a large spectrum pan-HDAC inhibitor (Selleckchem)) (Imai et al., 2016) for 24 h. DMSO was used as a control. Stimulation of human (100 μM) or mouse (10 μM) hepatocytes with Wy-14643 (DMSO used as a control) was done in combination with glucose stimulation (5 or 25 mM) 48 hours after seeding.

ChIP analysis

In vivo ChiP assays: Mouse liver tissue was submersed in PBS + 1% formaldehyde, cut into small pieces and incubated at room temperature for 15 minutes. Fixation was stopped by the addition of 0.125 M glycine (final). The tissue pieces were then treated with a TissueTearer and spun down and washed 2x in PBS. Chromatin was isolated by the addition of lysis buffer, followed by disruption with a Dounce homogenizer. Lysates were sonicated using the EpiShear™ Probe Sonicator (Active Motif, cat # 53051) with an

EpiShear™ Cooled Sonication Platform (Active Motif, cat # 53080) and the DNA sheared to an average length of 300-500 bp. Genomic DNA (Input) was prepared by treating aliquots of chromatin with RNase, proteinase K and heat for de-crosslinking (overnight at 65°C) followed by ethanol precipitation. Pellets were resuspended and the resulting DNA was quantified on a NanoDrop spectrophotometer. Extrapolation to the original chromatin volume allowed quantitation of the total chromatin yield. Aliquots of chromatin (30 μg) were pre-cleared with protein A or G agarose beads (Invitrogen). Genomic DNA regions of interest were isolated using antibodies against H3K9Ac (Active Motif, cat # 39917), RNA Pol II (Active Motif, cat# 39097), ChREBP (Novus, cat# NB400-135) and PPARα (Santa Cruz Biotechnologies, cat# sc-9000). Complexes were washed, eluted from the beads with SDS buffer, and subjected to RNase (20ug, 1 hour at 35°C) and proteinase K treatment (50μg, 3 hours at 35°C). Crosslinks were reversed by incubation overnight at 65°C, and ChIP DNA was purified by phenol-chloroform extraction and ethanol precipitation. QPCR reactions were carried out in triplicate using SYBR Green Supermix (Bio-Rad, Cat # 170-8882) on a CFX Connect™ Real Time PCR system. Positive and negative control sites were tested for each factor as well as the sites of interest. The resulting signals were normalized for primer efficiency by carrying out qPCR for each primer pair using input DNA (pooled unprecipitated genomic DNA from each sample). Specific enrichment was expressed as % of input.

In vitro ChiP assays from cultures hepatocytes were performed as previously described (Marmier et al. 2015). Proteins were cross-linked to DNA by addition of 1% formaldehyde for 10 minutes at room temperature. Crosslinking was stopped by a 5-minute incubation in 0.125 M glycine (final). Hepatocytes were scrapped and lysates were homogenized in low salt PIPES buffer and the nuclei fraction was enriched by a 10-

minute centrifugation. Sonication was performed in 10 seconds pulses, 15 times. Genomic DNA regions of interest were isolated using antibodies against ChREBP ChREBP (Novus, cat# NB400-135) and IgG (Cell Signaling). Immune complexes were captured with magnetic beads (Protein A-ChIP-Ademtech) and a saturated buffer. Positive and negative control sites were tested for each factor as well as the sites of interest. The resulting signals were normalized for primer efficiency by carrying out qPCR for each primer pair using input DNA (pooled unprecipitated genomic DNA from each sample). DNA fragments were quantified by qPCR, using primers described in Supplemental Table 1. Results are expressed in fold enrichment.

FAIRE qPCR

FAIRE qPCR was performed *Pparα*$^{hep+/+}$ and *Pparα*$^{hep-/-}$ hepatocytes using a protocol previously described (Simon et al., 2012). Cells were treated with 1% formaldehyde at room temperature for 5 minutes to form DNA-protein crosslinks and the crosslinking was stopped by addition of glycine to a final concentration of 125 mM. Cells were washed 3 times in 4°C PBS and lysed in cell lysis buffer (5mM PIPES, 85mM KCl, 0,5% NP40 and protease inhibitors) on ice for 10 minutes. Nuclei were pelleted and lysed in nuclei lysis buffer (50mM Tris, 10mM EDTA, 1% SDS and protease inhibitors) on ice for 10 minutes. Lysates were sonicated in a Bioruptor plus sonde (Diagenode). Cells debris was removed and DNA was extracted from supernatant by phenol/chloroform extraction. Under these conditions, DNA not crosslinked to proteins remains in the aqueous phase while the DNA cross-linked to proteins remains in the phenol phase. The FAIRE was analyzed by qPCR on genomic DNA using the ChoRE *Fgf21* primers (Figure 5C) and calculated by using relative enrichment for each amplicon using the comparative Ct method, such that a ratio is calculated for the signal from the FAIRE

sample relative to the signal from input control DNA. The results are expressed in fold enrichment.

References

Hozelberger, M, Lenzner, C., Leneuve, P., Zaoui, R.,Hammard, G., Vaulont, S., and Le Bouc, Y., (2000). Cre-mediated germline mosaicism: a method allowing rapid generation of several alleles on target genes. Nucleaic Acid Research. 28, e92.

Imai, Y. , Ohta, E.,Takeda, S., Sunamura, S., Ishibashi, M., Tamura, H., Wang, Y., Deguchi, A., Tanaka, J., Maru, Y., and Motoji, T. (2016). Histone deacetylase inhibitor panobinostat induces calcineurin degradation in multiple myeloma. JCI Insight;1(5):e85061.

Marmier, S., Dentin, R., Daujat-Chavanieu, M., Guillou, H., Bertrand-Michel, J., Gerbal-Chaloin, S., Girard, J., Lotersztajn S., Postic,C. (2015). Novel role for carbohydrate responsive element binding protein in the control of ethanol metabolism and susceptibility to binge drinking. Hepatology. 62(4):1086-100.

Montagner, A., Polizzi, A., Fouché, E., Ducheix, S., Lippi, Y., Lasserre, F., Barquissau, V., Régnier, M., Lukowicz, C., Benhamed, F., Iroz, A., Bertrand-Michel, J., Saati, T.A., Cano, P., Mselli-Lakhal, L., Mithieux, G., Rajas, F., Lagarrigue, S., Pineau, T., Loiseau, N., Postic, C., Langin, D., Wahli, W., and Guillou, H. (2016). Liver PPARα is crucial for whole-body fatty acid homeostasis and is protective against NAFLD. Gut 65(7):1202-1214.

Simon, J.M., Giresi, P.G., Davis, I.J., Lieb, J.D. (2012). Using formaldehyde-assisted isolation of regulatory elements (FAIRE) to isolate active regulatory DNA. Nat Protoc.;7(2):256-67.

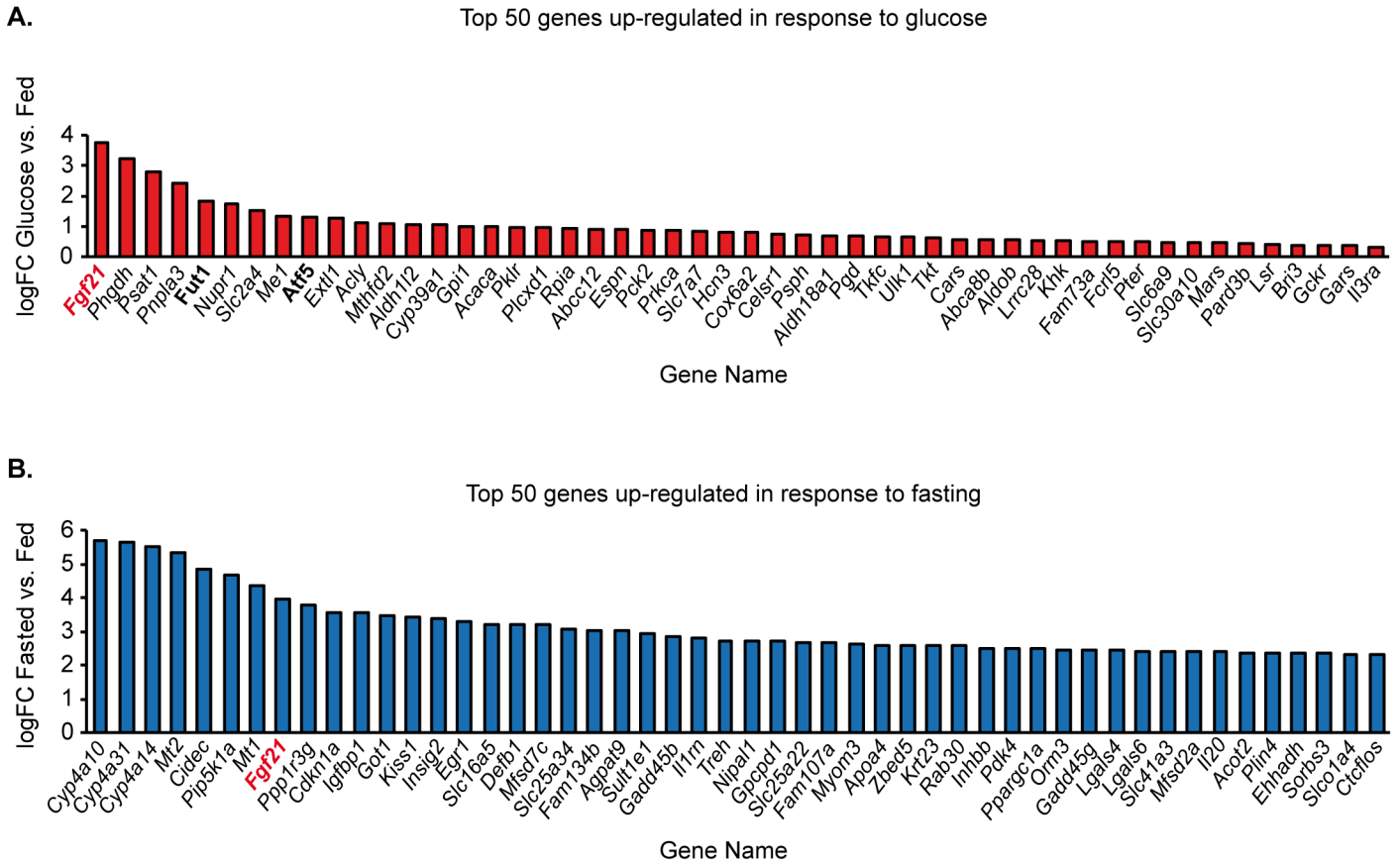

Figure S1. Related to Figure 1. Most significant induced genes in response to glucose and to fasting. (A) Microarray was performed and revealed that the top 50 genes showing up-regulation of mRNA levels in response to 24 hours glucose challenge (Glucose) when compared to fed mice (Fed). These genes were selected on the basis of significantly different mean of expression level (Glucose vs Fed, n=6 per group) with an adjusted p value <0.05. **(B)** Microarray was performed and revealed that the top 50 genes showing up-regulation of mRNA levels in response to 24 hours fasting (Fasted) when compared to fed mice (Fed). These genes were selected on the basis of significantly different mean of expression level (fasted vs Fed, n=6 per group) with an adjusted p value <0.05.

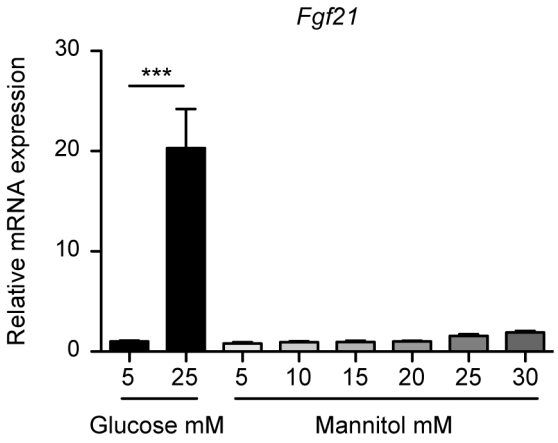

Figure S2. *Fgf21* is not induced by Mannitol in primary hepatocytes. Related to Figure 2. Primary hepatocytes derived from adult male C57BL/6J mice. Hepatocytes were stimulated one day after platting for 24 hours with medium containing 5, or 25 mM glucose; or increasing concentrations of mannitol (from 5 to 30 mM). Relative *Fgf21* gene expression was determined by qPCR. Data are presented as means ± SEM from 3 independent cultures. Each culture was completed in triplicate. Significance is based on 2-way ANOVA followed by Bonferroni post test, $p \leq 0.001$ (***).

A.

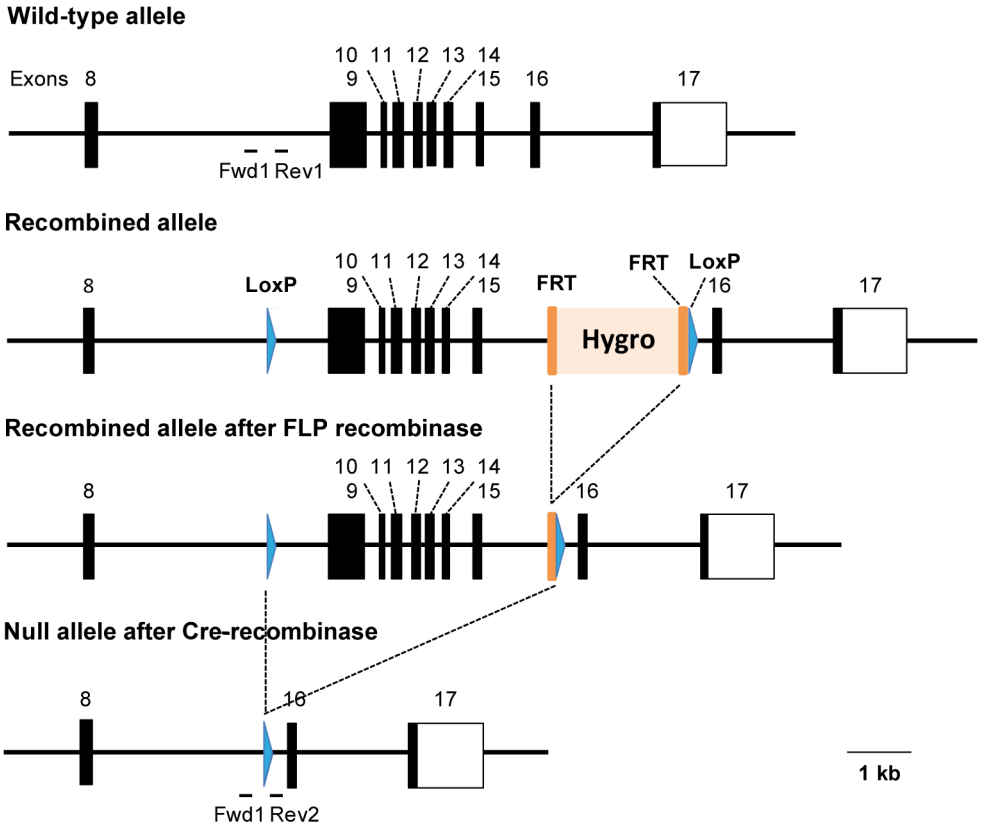

B.

Primer	*Sequence*	*Position*
Fwd1	CCACCCCTATGGAATGGTTC	Arm 5'
Rev1	GCACCCATTTACCAACTTAGTC	Floxable zone
Rev2	TCCCACATCTCTAGGCTCAG	Arm 3'

C.

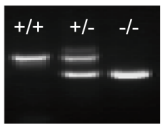

Figure S3. Generation of global ChREBP knockout mice. Related to Experimental procedures generation of knockout mice. Related to Figure 2. (A) Wild type and recombined alleles are indicated. Exons 9-15 were floxed to generate *Chrebp* conditional mutant allele. **(B)** PCR analysis was used to identify offspring that carry Cre-mediated recombination between *loxP1* and *loxP2* using primers Fwd1 and Rev1 for wild type allele: 319 bp and for the allele including *LoxP* site: 375 pb. Primer Fwd1 and Rev2: 477 bp were used for mutant allele. **(C)** The first lanes is a DNA sample from a wild type mice (+/+) detecting the 319 bp band, while the second lane is a DNA sample from a heterozygous mouse (+/-) detected the 375 bp band and the third lane is a *Chrebp* knockout mouse (-/-) detected at 477 bp band.

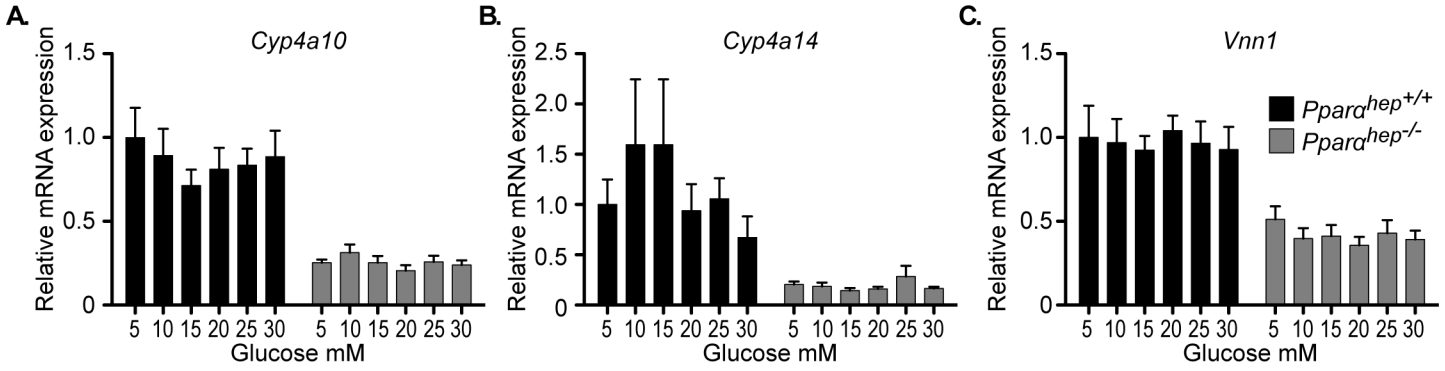

Figure S4. The expression of *Cyp4a10*, *Cyp4a14* and *Vnn1* is not induced by glucose. Related to Figure 4. Primary cultures of hepatocytes derived from adult male *Pparα*$^{hep+/+}$ or *Pparα*$^{hep-/-}$ mice. Hepatocytes were stimulated one day after platting for 24 hours with medium containing 5, 10, 15, 20, 25, or 30 mM glucose. Relative gene expression was determined by qPCR. Primers used were described in Montagner *et al.* 2016.

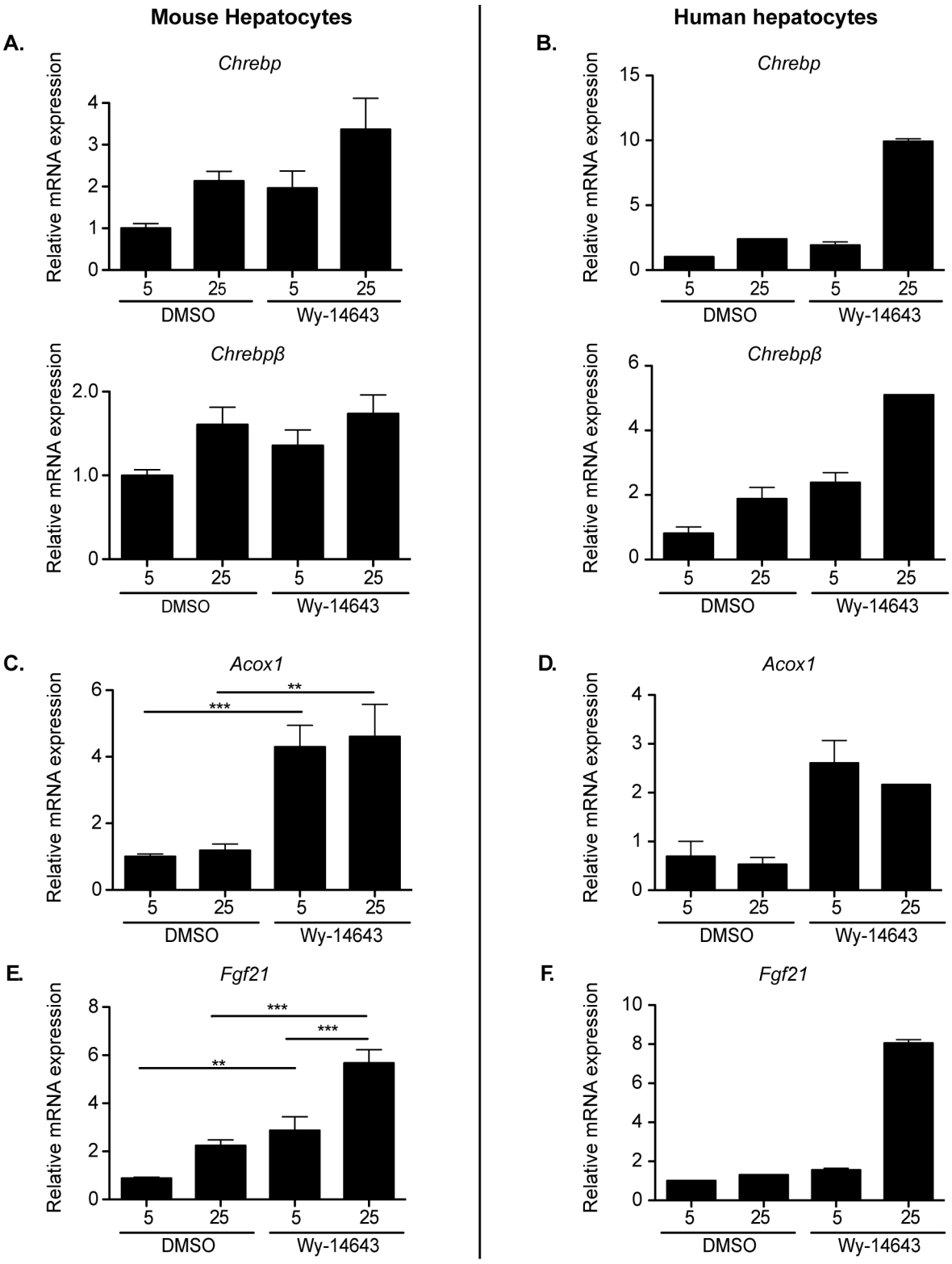

Figure S5. FGF21 synergistically responds to glucose and a pharmacological PPARα activator in both mouse and human hepatocytes. Primary mouse **(A-E)** or human hepatocytes **(B-F)** stimulated 24 hours with medium containing 5 or 25 mM glucose and of 100 µM Wy-14643, 10 µl of DMSO was used as a control. Relative gene expression was determined by qPCR. Mouse data are presented as means ± SEM from 4 independent cultures. Each culture was completed in triplicate. Significance is based on 2-way ANOVA followed by Bonferroni post test $p \leq 0.01$ (**), $p \leq 0.001$ (***). Human hepatocyte data are presented as means ± SEM from 1 culture in triplicate assays.

Table S1. Primers used for qPCR ChIP analysis. Related to Figure 2

Mouse Genes		Sequences for ChIP	T fusion °C
ChoRE *Fgf21*	forward	TAGCCCTTTTCATTCAGCCCCT	60
	reverse	CTCTGTGTTGAACTCCCAGCTGA	
ChoRE *L-pk*	forward	GTCCCACACTTTGGAAGCAT	60
	reverse	CCCAACACTGATTCTACCC	

Table S2. Primers used for qPCR analysis of mouse mRNA. Related to Figures 1 to 6.

Mouse Genes		Sequences for qPCR	T fusion °C
ChREBP	forward	AATGGGATGGTGTCTACCGC	58
	reverse	GGCGAAGGGAATTCAGGACA	
ChREBP β	forward	TCTGCAGATCGCGTGGAG	58
	reverse	CT GTCCCGGCATAGCAAC	
L-pk	forward	CTTGCTCTACCGTGAGCCTC	58
	reverse	ACCACAATCACCAGATCACC	
Scd1	forward	CCGGAGACCCCTTAGATCGA	58
	reverse	TAGCCTGTAAAAGATTTCTGCAAA	
Fgf21	forward	TACAATGTGTACCAGTCTGAAG	58
	reverse	ACAGCCCTAGATTCAGGA	
Acox1	forward	CCGCCTATGCCTTCCACTTTC	60
	reverse	CAAGCCATCCGACATTCTTCG	
TBP	forward	CCCCACAACTCTTCCATTCT	58
	reverse	GCAGGAGTGATAGGGGTCAT	

Table S3. Primers used for qPCR analysis of human mRNA. Related to Figure S5.

Human Genes		Sequences for qPCR	T fusion °C
ChREBP	forward	CCA GCC TCA AGG TGA GCA AA	58
	reverse	CAC GCT CCT GCT GTA GCA	
ChREBP β	forward	AGCGGATTCCAGGTGAGG	58
	reverse	TTGTTCAGGCGGATCTTGTC	
L-pk	forward	TGGGCCTCATGCCTCTGACA	58
	reverse	TCCTGGGTCAGTTGGGCCAC	
Fgf21	forward	GGATTCGGACTGGTAAACAT	58
	reverse	GGGAGTCAAGACATCCAGGT	
Acox1	forward	GTGGGCTTGGAAAGACTTCA	58
	reverse	CCGATGTCACCAACGGTAAT	
18S	forward	CCATCCAATCGGTAGTAGCG	58
	reverse	GTAACCCGTTGAACCCCATT	